Recurrent magnetic dipolarization at Saturn: revealed by Cassini

Z. H. Yao[1], A. Radioti[1], D. Grodent[1], L. C. Ray[2], B. Palmaerts[1], N. Sergis[3,13], K. Dialynas[3], A. C. Coates[4], C. S. Arridge[2], E. Roussos[5], S. V. Badman[2], Sheng-Yi Ye[6], J.-C. Gérard[1],P. A. Delamere[7], R. L. Guo[8], Z. Y. Pu[9], J. H. Waite[10], N. Krupp[5], D. G. Mitchell[11] and M. K. Dougherty[12]

[1]Laboratoire de Physique Atmosphérique et Planétaire, Space sciences, Technologies and Astrophysics Research (STAR) Institute, Université de Liège, Liège, Belgium
[2]Department of Physics, Lancaster University, Bailrigg, Lancaster LA1 4YB, UK
[3]Office for Space Research and Technology, Academy of Athens, Athens, Greece
[4]UCL Mullard Space Science Laboratory, Dorking, RH5 6NT, UK
[5]Max Planck Institute for Solar System Research, Göttingen, Germany
[6]Department of Physics and Astronomy, University of Iowa, Iowa City, IA 52242, USA
[7]Geophysical Institute, University of Alaska Fairbanks, Fairbanks, Alaska, USA
[8]Institute of Geology and Geophysics, Chinese Academy of Sciences, Beijing, China
[9]School of Earth and Space Sciences, Peking University, Beijing 100871, China
[10]Southwest Research Institute, San Antonio, TX, United States
[11]Johns Hopkins University Applied Physics Laboratory, Laurel, MD 20723, USA
[12]Faculty of Natural Sciences, Department of Physics, Imperial College, London, UK
[13]Institute of Astronomy, Astrophysics, Space Applications and Remote Sensing, National Observatory of Athens, Athens, Greece

Key Points:

- We report a recurrent type of magnetic dipolarization at Saturn.
- The associated processes could efficiently accelerate electrons and ions to 10s-100s keV.
- Corotation of magnetosphere and planetary periodic oscillation are suggested as possible mechanisms.

Corresponding author: Zhonghua Yao, `zhonghua.yao@uliege.be`

Abstract

Planetary magnetospheres receive plasma and energy from the Sun or moons of planets, and consequently stretch magnetic field lines. The process may last for varied time scales at different planets. From time to time, energy is rapidly released in the magnetosphere, and subsequently precipitated into the ionosphere and upper atmosphere. Usually, this energy dissipation is associated with magnetic dipolarization in the magnetosphere.This process is accompanied by plasma acceleration and field-aligned current formation, and subsequently auroral emissions are often significantly enhanced. Using measurements from multiple instruments onboard the Cassini spacecraft, we reveal that magnetic dipolarization event at Saturn could reoccur after one planetary rotation, and name them as recurrent dipolarization. Three events are presented, including one from the dayside magnetosphere, which has no known precedent with terrestrial magnetospheric observations. During these events, recurrent energisations of plasma (electrons or ions) were also detected, which clearly demonstrate that these processes shall not be simply attributed to modulation of planetary periodic oscillation, although we do not exclude the possibility that the planetary periodic oscillation may modulate other processes (e.g., magnetic reconnection) which energises particles. We discuss the potential physical mechanisms for generating the recurrent dipolarization process in a comprehensive view, including aurora and energetic neutral atom emissions.

1 Introduction

In Saturn's magnetosphere, sources of energy and plasmas include the solar wind ejected from the Sun, moons and rings embeded within the system, and the planetary atmosphere [*Blanc et al.*, 2015]. Energy loading processes occur when electrical currents driven by plasma dynamics reshape the magnetosphere from its steady-state configuration. During the loading process, the planetary magnetic field becomes stretched, which corresponds to the formation of ring currents on the magnetodisc [*Arridge et al.*, 2008]. Both the solar wind and rapid planetary rotation can drive such energy loading processes, with the rapid planetary rotation usually loading energy much faster than solar wind processes [*Yao*, 2017].

Magnetospheric dynamics often produce a rapid energy release from Saturn's magnetosphere, which subsequently drives particle precipitation into the ionosphere and upper atmosphere of Saturn [*Kivelson*, 2005]. The rapid energy dissipation perturbs the current system in both the magnetosphere and ionosphere, reconfiguring the magnetospheric magnetic field, powering aurorae in the atmosphere. The magnetospheric and ionospheric phenomena are physically connected by field-aligned currents [*Talboys et al.*, 2009; *Bunce et al.*, 2010; *Schippers et al.*, 2012] and field-aligned accelerated ions and electrons [*Saur et al.*, 2006; *Mitchell et al.*, 2009a,b; *Yao et al.*, 2017a]. The magnetic field reconfiguration in the magnetosphere is well known as magnetic dipolarization, i.e., the magnetospheric currents divert into the ionosphere, and thus the dipole magnetic field from the planet dominates the near planet space. The dipolarization process has been reported at Earth [*Hesse and Birn*, 1991; *Lui*, 1996; *Angelopoulos et al.*, 2008], Mercury [*Slavin et al.*, 2010], Saturn [*Jackman et al.*, 2007] and Jupiter [*Kronberg et al.*, 2005]. However, it is not always easy to distinguish between a magnetic field change caused by the global current diversion from the magnetosphere to the ionosphere [*McPherron et al.*, 1973] and the magnetic field modified by a local current system [*Yao et al.*, 2013] from in-situ data. Moreover, *Yao et al.* [2017b] demonstrated that there are two fundamentally different processes that can produce the dipolarization-like magnetic signature at both the Earth and Saturn, while only the global current diversion is expected to produce a global scale intensification of aurora.

Saturn's magnetosphere also rapidly rotates [*Espinosa et al.*, 2003], which naturally impose the spatial variations of magnetic field in azimuthal direction on the the in-situ measurements from spacecraft. Because Saturn's magnetosphere is rotating, a spacecraft would naturally measure longitudinal variation. The longitudinal variation could be any component of the magnetic field. Moreover the measured magnetic field could also be modulated by planetary periodic oscillation (PPO) [*Espinosa and Dougherty*, 2000; *Cowley et al.*, 2006]. The two systematic effects do not exist at terrestrial magnetotail, in which region the dynamics are usually compared with giant planets. Two PPO-related current systems (northern and southern hemispheres) combine together to modulate Saturn's magnetodisc [*Andrews*, 2011; *Provan et al.*, 2012; *Hunt et al.*, 2015], and thus produce sinusoidal variation of magnetic fields or periodic crossings of the magnetospheric current sheet [*Arridge et al.*, 2011]. In addition to the dual rotating current systems, *Brandt et al.* [2010] reveal that the electrical currents driven by the asymmetric pressure distribution composed of energetic particle distributions can also produce similar planetary periodic magnetic perturbations.

Regarding that many planetary modulations of magnetic fields are absent at Earth, analogy of magnetic signatures (e.g., magnetic dipolarization, magnetic islands etc.) is not straightforward. Fundamentally different magnetospheric dynamics between Saturn and Earth are also reflected in their very different auroral dynamics. At Earth, auroral enhancements are usually very explosive (i.e., at a time scale of a few minutes) [*Lui et al.*, 2008; *Henderson*, 2009], while at Saturn the enhancements can last for a few hours [*Nichols et al.*, 2014; *Radioti et al.*, 2016]. Besides the different time scales, previous studies also clearly demonstrate that Saturn auroral breakup region is rotating along Saturn's spin direction, which is fundamentally different from auroral breakup at Earth [*Akasofu*, 1964]. Most likely the rotating of Saturn's auroral breakup region would require a rotating field-aligned current system and a rotating precipitating magnetospheric source.

The precise connection between auroral dynamics and magnetospheric dynamics at Saturn remains poorly understood. A major reason is the high variability of both auroral morphology and magnetospheric dynamics, particularly in the high latitude polar region and their magnetospheric counterpart [*Grodent et al.*, 2005; *Stallard et al.*, 2008; *Radioti et al.*, 2014, 2015; *Mitchell et al.*, 2016]. The highly dynamical auroral emissions are associated with the formation of field-aligned current system that couples the magnetosphere and the ionosphere [*Bunce et al.*, 2008; *Yao et al.*, 2017b], as well as plasma waves in the magnetosphere (e.g., *Yao et al.* [2017c]). In addition to these high variabilities, *Badman et al.* [2006] present strong dawn-dusk asymmetry of auroral intensity, which strongly evidence the impact of solar wind.

Regarding the many differences in magnetospheric environments and auroral dynamics at Saturn and Earth, many similarities of fundamental plasma processes still exist at these planets, e.g., magnetic reconnection and dipolarization. For example, similarities of magnetic dipolarization process have often been reported, including particle acceleration [*Arridge et al.*, 2016; *Yao et al.*, 2017b; *Smith et al.*, 2018], field-aligned current formation [*Jackman et al.*, 2013, 2015], planetward bursty flow [*Thomsen et al.*, 2014] and tailward plasmoid phenomena [*Jackman et al.*, 2011]. It is intriguing to identify both the similarities and differences in the magnetosphere-ionosphere coupling processes between both planets. In this paper, we report recurrent magnetic dipolarization events at Saturn. The dipolarization process at Saturn is similar to the terrestrial dipolarization, while the recurrent feature is unknown at Earth. We also reveal the plasma features associated with these recurrent dipolarization events, and discuss their potential mechanisms by taking into account of results from multiple datasets (i.e.,, magnetic fields, ions and electrons at different energies, aurorae, energetic neutral atom (ENA)). Their potential relations to ENA and auroral enhancements are also discussed in this study.

2 Observations

In this section, we detail three recurrent dipolarization events (note that each recurrent dipolarization includes two individual dipolarization events separately by about one planetary rotation period) at Saturn with observations made by multiple instruments onboard the Cassini spacecraft. In the Cassini dataset, we do not identify a dipolarization that appeared three times in succession, which could due to two possible reasons, 1) the recurred dipolarization is a persist structure that corotates with the planet and has a lifetime of less than two planetary rotations, 2) within two planetary rotations, Cassini would travel a relatively large distance, and therefore not likely to measure a structure with limited spatial scale more than twice. From the periodic nature of ENA revealed in previous studies [*Brandt et al.*, 2010; *Mitchell et al.*, 2009a], we intend to suggest the second reason in this study, although we could not exclude the possibility of the first situation. Cassini-MAG [*Dougherty et al.*, 2004] provides magnetic field. Cassini-CAPS onboard Cassini [*Young et al.*, 2004] provide low energy electron measurements with the CAPS-ELS detector and ion measurements with the CAPS-IMS detector. The energetic particle data used in this paper were collected by the Low Energy Magnetospheric Measurement System (LEMMS) of the Magnetosphere Imaging Instrument (MIMI) [*Krimigis et al.*, 2004]. The auroral images of Saturn's polar region were obtained from the UVIS spectrograph [*Esposito et al.*, 2004].

2.1 Recurrent dipolarization event 1: 07 August 2009

Figure 1 shows the overview of the magnetic fields and plasma data observed by the Cassini spacecraft on 07 August 2009. The 1-min resolution magnetic fields shown in Figure 1(a-c) are provided in Kronographic Radial-Theta-Phi (KRTP) coordinate system. This is a Saturn-centered coordinate: radial vector r is directed from Saturn's center to the spacecraft, the azimuthal component ϕ is parallel to the direction of corotation and the southward θ completes the right-hand set. Figure 1d and 1e show the differential electron energy flux measured by the CAPS-ELS detector and differential ion energy flux from the CAPS-IMS Singles (SNG) data product. Figure 1f and 1g shows electron and ion counts fluxes at higher energies measured by MIMI instruments. During this period, Cassini was located pre-midnight between 20.6 and 20.9 Saturn local time (SLT), at latitudes from ~ 9°N to 11°N north of Saturn's equatorial plane and at radial distance from R ~ 30 to 32 R_S (1 R_S = 60268 km). Magnetic fields show clear planetary period oscillation (PPO) (please see the supporting document S1 for a longer period of magnetic field, which has been discussed in previous literature (e.g., *Clarke et al.* [2006], *Cowley et al.* [2006], *Andrews et al.* [2012], [*Provan et al.*, 2018]). On top of the regular magnetic PPO, we notice two distinctive B_r decreases from ~3 nT to ~2 nT (marked by the vertical dashed black lines). The separation between these two B_r decreases is 11 hours, almost exactly a planetary rotation period. We therefore call them recurrent dipolarization events, following similar descriptions (e.g., recurrent acceleration events) used in *Mitchell et al.* [2009a]. The first B_r decrease was accompanied by B_θ increase from ~1 nT to ~ 2 nT. Meanwhile, enhancement of electron flux was also observed during the two B_r decrease periods. These are typical signatures of magnetospheric current re-distribution dipolarization (CRDD), as defined in *Yao et al.* [2017b]. More details on this event can be found in *Yao et al.* [2017b]. In the present study, our major focus is the long-term view of the dipolarization process, and the associated energetic particles. It is important here to remind that the identification of dipolarization must rely on both the decrease of B_r and the increase of B_θ. B_r decrease is more indicative when a spacecraft is in the outer plasma sheet, while increase of B_θ usually serves as a good indicator when spacecraft is near the central current sheet. Plasma energisation could serve as a good indicator to determine whether a process is dipolarization or a pure current sheet flapping [*Yao et al.*, 2017d]. In our study, we clearly notice a large B_r during the whole period, therefore we would need to treat B_r as the key indicator of a dipolarization process. To distinguish between the two dipolarization processes, we named the dipolarization observed at ~ 01:50 UT as DP1 (the first vertical dashed black line), and the one observed at ~ 12:50 UT as DP2 (the second vertical dashed black line). For DP1 and DP2, Cassini ion instruments did not record any significant flux enhancements with energies from a few eV to hundreds keV. However, electron fluxes were enhanced with energies from ~ 100 eV to ~ 500 keV.

In Figure 2, we compare the measured magnetic fields from DP1, DP2 and the measurements from one rotation prior to DP1 that could set as a baseline. The three 8h-periods are marked by the blue (2009 August 06/13:00 UT to 21:00 UT), black (2009 August 07/00:00 UT to 08:00 UT) and red (2009 August 07/11:00 UT to 19:00 UT) patches at the top of Figure 2a. As shown in Figure 2b, a general consistent trend in the magnetic field's main component B_r is obvious for the three periods. During the baseline period (blue curve), B_r component changes smoothly, which includes effects from both the PPO's modulation and magnetosphere's rotation. Comparing to the baseline variation, the most significant differences of B_r during DP1 and DP2 periods exist between T_0 + 1 h and T_0 + 5 h. For the decrease of B_r, the magnitudes of decrease and the time scales were remarkably similar. The recurrent dipolarization event (DP1 and DP2) is significantly different from background variation (blue dashed curve in Figure 2b), and the two dipolarization events look like very localised structures since the variation return to background profile rapidly. Therefore the recurrent dipolarization event is clearly different from the PPO's modulation of long-term scale variation. Moreover, electrons shown in Figure 1g were accelerated up to ~ 500 keV, strongly evidence that there was an efficient acceleration accompanying these structures, instead of a pure modulation process.

2.2 Recurrent dipolarization event 2: 06 February 2009

Figure 3 presents overview of another recurrent dipolarization event observed on 06 February 2009 with the same format as Figure 1. This event was detected one day prior to Cassini's Titan flyby (T-50), when Cassini was outbound traveling from R ~ 18.7 to 19.6 R_S, at latitudes from ~ $-25°$ to -7° south of Saturn's equatorial plane, and at pre-noon from 9.5 to 10 SLT. Similar to event 1, a clear PPO modulation of magnetic fields is shown in Figure 3(a-c) (please see the supporting document S2 for a longer period of magnetic field. The two dashed vertical lines indicate two B_θ enhancements, accompanied by B_r decreases. As shown in Figure 3d and 3e, ~ 1 keV ions and few hundreds eV electrons were observed prior to the two dipolarization, indicating that the Cassini spacecraft was in the central plasma sheet but not at its outer boundary or in the lobe region (the case of Event 1).

As shown in Figure 3d and 3f, ion fluxes are enhanced at energies from ~ 1 keV to ~ 200 keV, which is significantly different from the Event 1. It is unclear whether this difference is caused by different locations (i.e., inner and outer current sheet), or due to different acceleration mechanisms. During the dipolarization processes, ambient electrons with energies at a few hundreds of eV were sufficiently accelerated to a few keV (Figure 3e). Moreover, energetic electrons with energy up to 500 keV were also significantly enhanced. For the energetic ions (Figure 3f, mostly protons) and electrons (Figure 3g), a pulsation (1-2 hours) that has been often identified in Saturn's magnetosphere (e.g., *Roussos et al.* [2016] and [*Palmaerts et al.*, 2016]), was clearly identified for the first dipolarization, while was absent for the second one. The pulsations of electrons and ions were also detected at energies of a few keV by the CAPS instruments (Figure 3d and e). It is unclear whether the absence of pulsation in the second dipolarization is due to a different plasma process or not. There is a boundary likely associated with spatial variation as marked by the purple vertical line, which might be associated with the approaching to Titan. This boundary can be seen clearly from all three field components, indicating that the field has a markedly different character. Although no literature that we are aware of has explained why the approaching to Titan could produce dropout of plasma fluxes, we have identified many similar feature during other Cassini's other approaches to approach Titan. Since it is not a major scope of the present study, we do not go further into Titan's interaction with Saturn's magnetosphere in this research.

2.3 Recurrent dipolarization event 3: 19 September 2010

Event 3 was observed on 19 September 2010, when Cassini was located post-evening at $\sim$ 20 SLT, near-equator with latitudes at $\sim -4°$ south hemisphere and at radial distance from R $\sim$ 32 to 29 R_S. As demonstrated in *Thomsen et al.* [2017], PPO modulation of magnetic fields often shows asymmetries between northbound and southbound crossings in 2010. The asymmetric PPO modulation signature is clearly presented in Figure 4(a-c) (please see the supporting document S3 for a longer period of magnetic field), i.e., the north to south crossings were much more rapid than south to north crossings (or B_r positive to negative changing was quicker than negative to north changing). Within the large-scale modulation, rapid enhancements of B_θ were observed at the trailing phase of each period, which was also accompanied by short-duration wiggle structures in B_r and B_ϕ components. The two distinctive B_θ enhancements are separated by about 10.7 hour, almost a planetary rotation. Since the spacecraft was very close to the equator (indicated by the small latitude and small B_r), therefore the variation of B_θ shall be considered as the most important indicator, which is very different from the situation when a spacecraft was in outer current sheet, for example in event 1.

As shown in Figure 4d and 4e, ions and electrons remained roughly at ambient energies. The fluxes of electrons and ions were enhanced for the first dipolarization, while no significant during the second dipolarization for this recurrent event. The ion counts shown in Figure 4f show slight enhancements associated with the two dipolarization periods at relatively low energy channels (< 100 keV). From Figure 4g, we also see that there was a very slight enhancement in energetic electrons with energies below 100 keV. The pulsating enhancements of energetic electrons between 14 UT to 16 UT are likely associated with the rotation of spacecraft during this period. From the electron flux shown in Figure 4e, we do not see clearly energisation of electrons and sharp boundary to distinguish between the pre-dipolarization and after dipolarization populations, therefore we could conclude that the pair of dipolarization events are current redistribution dipolarization rather than dipolarization front as defined in *Yao et al.* [2017b].

In this event, Cassini was relatively close to the central plasmadisc, and was able to provide ion velocity components, as shown in Figure 4h. The pair of dipolarization events were accompanied with significant bulk flow in the planetary corotating direction. The peak flow velocity for the first dipolarization was about 360 km/s, and for the second was about 250 km/s. The both velocity are very close to the rigid corotating velocity (∼ 300 km/s), and the greater than planetary rotating velocity during the first dipolarization is also been explained as supercorotating return flow from reconnection in Saturn's magnetotail [*Masters et al.*, 2011]. The relation between fast plasma flow and magnetic dipolarization is very complicated and remains controversial even by combining multiple datasets from multi-probe mission and ground stations in terrestrial research [*Keiling et al.*, 2009; *Yao et al.*, 2012]. Since their relation is not one major focus of this paper, we therefore do not go further on this point.

3 Discussion

Magnetic reconnection, substorm dipolarization, current disruption and field-aligned current formation are strongly coupled processes. At Earth these processes usually take place in nightside magnetotail, with a preference at pre-midnight local time [*Runov et al.*, 2017]. In giant planetary magnetospheres, internal drivers usually dominate magnetospheric dynamics, and would lead to a preference during post-midnight local times [*Vasyliunas*, 1983]. The survey of dipolarization events in the nightside magnetosphere also revealed higher occurrences during post-midnight [*Smith et al.*, 2018]. Although previous investigations on magnetic dipolarization are restricted to the nightside magnetosphere, it may need to be updated, since the magnetic reconnection process that is strongly coupled to dipolarization has been recently proposed by *Delamere et al.* [2015] and observed by *Guo et al.* [2018] to take place in Saturn's dayside magnetodisc.

Bend back configuration of magnetic field is an expected feature produced by net mass outflow, and bend forward configuration is expected to follow magnetic reconnection. By surveying bend forward magnetic configuration from 2004 to 2012 with Cassini-MAG instrument, *Delamere et al.* [2015] revealed that reconnection could take place in all local times. Furthermore, they show high probabilities of reconnection at postnoon sectors, and proposed "drizzle-like" process to explain their observations. Furthermore, *Guo et al.* [2018], using Cassini in-situ measurements, identified the reconnection associated Hall current system and reconnection accelerated plasma (including electrons and ions) in near-noon magnetodisc for the first time. *Guo et al.* [2018] also detailed that the reconnection produced acceleration of heavy ions, and pulsating energetic electrons. Following these studies, we would naturally expect magnetic dipolarization process to exist in Saturn's dayside magnetosphere. In this study, event 2 was observed at about 10 SLT, which further evidences that the internal processes are important in driving dayside magnetospheric dynamics, and demonstrates that magnetic dipolarization processes to exist in Saturn's dayside.

The recurrent nature of dipolarization is very intriguing, leading to many open questions. One of the major difficulties is to distinguish between spatial variation and temporal variation from single spacecraft's in-situ measurements. The recurrent magnetic dipolarization events could be detected if a dipolarized region corotates with Saturn, or explained as a not yet known PPO-modulated phenomenon. Each of them also has fundamental difficulties to be compatible with some previous observations.

3.1 Implications from the rotation of auroral breakup sites and ENA emissions at Saturn

A natural explanation for recurrent phenomena would be corotation of magnetospheric sources. If a dipolarized region could corotate with the planet, we could then expect to measure the same structure after one planetary rotation. This would also perfectly explain why DF1 and DF2 in event 1 are so consistent, as shown in Figure 2b. Moreover, rotation of magnetospheric sources (e.g., ENA enhancements) and their consequent aurorae has been extensively studied. The rotation of magnetospheric source at up to 30 R_S

in the night would cause a mystery: what would happen when the source experiences the dayside interaction? Besides the current system in the magnetodisc, the chapman-Ferraro current system on magnetopause induced by solar wind can also make the magnetosphere asymmetric. The magnetopause current leads to a day-night asymmetry in the magnetosphere, indicating that the magnetic field lines extend farther from the planet at the nightside than the dayside (similar to the Earth, see Figure 1 in *Hones* [1963]). Therefore, due to the aforementioned asymmetry and the asymmetric flow patterns inside the magnetosphere (e.g., *Dialynas* [2018] and *Allen et al.* [2018]), the events that are discussed in the present study could naturally remain inside the magnetopause at a closer distance when they reach the dayside. the first event (on 7 August 2009) was observed at about 30 R_S in postdusk sector, we could also expect the site to remain in the magnetosphere following the dawn-dusk asymmetry revealed by *Pilkington et al.* [2015], who showed from Cassini's large dataset that the magnetosphere extends farther from the planet on the dawnside of the planet by 6% to 8%. Since there is no similar modeling study that we are aware of at Saturn as Hones 1963 performed for the Earth, we could not quantify the dayside location that corresponds to the nightside at 30 R_S.

Subcorotation of aurora at Saturn has been reported in previous research. Using measurements from Hubble Space Telescope, *Grodent et al.* [2005] showed that the bulk auroral emission region is rotating at 65% ± 10% of the angular velocity of rigid planetary rotating velocity. Angular velocity for some extreme isolated auroral structures constantly decreases with time, down to 20° per hour. Similar evidence that aurora sub-corotates with planet has also been provided by measurements from Cassini-UVIS instrument (e.g., *Radioti et al.* [2014] and *Mitchell et al.* [2016]).

To demonstrate how auroral breakup region rotates, we here quantify the angular rotating velocity of a typical auroral intensification event on DOY 129, 2008, which has also been discussed in detail by *Mitchell et al.* [2016]. The aurora sequence consists of 24 images, from 08:08 UT to 13:39 UT. We specifically focus on a distinctive dawnside auroral intensification from 08:53 UT to 11:53 UT. A sequence of auroral images is shown in Figure 5a, with 1-hour separation between them. It is clear that the auroral patch was rotating and enhanced (also expanded) during this sequence. We need to point out that there is no perfect method to quantify the rotating angular velocity for such a dynamic structure. In this study, we provide an empirical method to quantify potential lower and upper limits of the rotating angular velocity. We integrate aurora intensity over latitude between 68 deg to 76 deg (indicated by the two ocher circles), and obtained an intensity distribution along local time for each image, as shown in Figure 5b. From 08:53 UT to 11:53 UT, the intensity has clearly enhanced, and distributed in a wider local time range, with an obvious bulk shift in local time. In Figure 5c, we add an angular velocity of 1.2 SLT per hour (SLT/h) for the profiles of 08:53 UT, 09:53 UT and 10:53 UT, and obtain a consistency in the trailing edge (i.e., low local time) of these profiles of enhanced aurora intensity for the four given times, to be compared with the profile at 11:53 UT. Similarly, if we add a rotating angular velocity of 1.5 SLT/h for these profiles, we can find a good consistency on their leading edges (i.e., high local time) in Figure 5d, with the exception for the 08:53 UT profile. The 08:53 UT profile shows a similar center to other profiles in Figure 5d. The 08:53 auroral intensification was limited in a much narrower region than the other three, and therefore we shall not aim to match the boundary of 08:53 UT profile to determine a rotating velocity. From Figure 5c and 5d, we suggest that the rotating angular velocity of this auroral intensification region was from 1.2 to 1.5 SLT/h, i.e., 53% to 66% of the rigid planetary rotating angular velocity. This result is consistent with the multicase statistical results in *Grodent et al.* [2005].

Auroral intensification has also been found to co-exist with enhancement in ENA emission at the same local time [*Mitchell et al.*, 2009a], which provides a stronge evidence that the ENA emission is likely associated with the magnetospheric source of aurorae. Their results may suggest either that the ENA region is the source for aurora, or that the ENA enhancement and aurora are two individual consequences of the same magnetospheric dynamics. Therefore, dipolarization, enhancement of the ENA emission is strongly connected with auroral enhancements, which is believed to be associated with magnetic dipolarization, and they likely represent three different views of the same magnetosphere-ionosphere coupling dynamics. ENAs are charge-exchange products between fast ions and background neutral gas populations, resident in Saturn's magnetosphere (mainly sourced from Enceladus water vapor plumes [*Waite et al.*, 2006]). It is important to have in mind that ENAs carry not only spectral information, but also compositional information of the source plasma, i.e. are always of the same species as their parent ion population, independently of the target neutral gas distribution and therefore, they can be considered as long distance communicators of the processes that their parent ion distributions undergo (e.g. *Dialynas et al.* [2013], for details).

Auroral intensification region for the event presented in this study rotates with 53% to 66% of planetary rotating velocity, which is also in consistency with previous studies. The enhanced ENA emission on average rotates at angular velocity ranging from ~ 28°/h at 5 R_S to ~ 21°/h between 10 and 20 R_S, corresponding to 85% and 64% of rigid corotation [*Carbary and Mitchell*, 2014]. We also notice that it is difficult to determine rotating velocity of enhancement of ENA emission for individual events, as the shape of ENA emission is usually very dynamic. However, the angular velocity for long-duration ENA potentially can be accurately determined. For example, if an ENA event lasts for one planetary rotation, then a shape change of 1-2 hours in local time would only involve an uncertainty of less than 10%. On average, ENA emissions are found to subcorotate with planet without distinguishing the different mechanisms generating these ENA emissions. However, rigidly corotating ENA emission enhancement can also often be identified, for example, *Krimigis et al.* [2007] present a rigidly corotating ENA emission event that lasted for longer than one planetary rotation, which is associated with enhanced partial ring currents. Other near corotating ENA emission enhancement events can also be found from the online dataset (`http://cassini-mimi.jhuapl.edu/PDS_Volumes/COMIMI_I001/BROWSE/`)

Many potential mechanisms may lead to enhancements of ENA emissions in Saturn's magnetosphere (e.g., enhancement of partial ring currents [*Krimigis et al.*, 2007], plasma injection [*Mauk et al.*, 2005] and Titan's interaction with Saturn's magnetosphere [*Mitchell et al.*, 2005]), and probably different mechanisms would produce different angular velocities. Moreover, the ENA angular velocity may evolve during the rotation, since it would constantly interact with the electromagnetic environment. Here we speculate that the ENA emission enhancements associated with dipolarization process would have high rotating velocity, and may even rigidly corotate with the planet. Besides ENA emission, we also propose a physical picture to connect the corotating dipolarized region and subcororating auroral intensification, which is illustrated in Figure 6. A corotating dipolarized site, as indicated by the blue lines in Figure 6a, rotates from 0h LT to 24h LT every planetary rotation period, and can be observed by an observer (the green arrow on the left) only once during each rotation. Note that here we assume that the observer's position does not significantly change in latitude and local time in the time scale of planetary rotation period, which is the case for Cassini spacecraft in the magnetosphere at the time to make observations that we used in this study. The orange cloud in Figure 6a illustrates how the local time position of the aurora intensification site changes with time.

Unlike the enhanced ENA emissions or dipolarization process that could last for longer than one planetary rotation period, auroral intensification structure usually decays in a few hours. This is understandable, as auroral intensification are generally caused by enhanced electron precipitations, which would disappear after a few electron bouncing periods if no new source fills in the loss cone of the particle distributions when the energy source of aurora is exhausted. ENA emission suggests trapped energetic particles in the magnetosphere and dipolarization suggests a relaxed state of the magnetosphere. The trapped energetic population could exist much longer time than the transient auroral emissions. The transient auroral intensification usually suggest an enhancement of electron precipitation and formation of field-aligned currents, which is a consequence of magnetospheric currents diversion into the ionosphere. During this process, azimuthal magnetic field component is expected to decrease, and to form a sharp spatial gradient that corresponds to formation of field-aligned currents [*Balogh et al.*, 1992; *Cowley et al.*, 2008]. The rapid decrease in azimuthal component B_ϕ would produce a change of magnetic geometry, and hence would change the footpoint of magnetospheric source in the ionosphere. Therefore, during a transient process like magnetic dipolarization that involves field-aligned current formation, the footpoint of magnetospheric site would move in azimuthal direction, meaning that conjugated sites in the magnetosphere and ionosphere could rotate at different angular velocity.

As illustrated in Figure 6b, the magnetic field line in equatorial plane would change from the black curve to the red curve, and therefore the footpoint of the magnetospheric source would drift opposite to planetary rotation. In below description, the subscript *ms* refer to the magnetosphere, and ion refer to the ionosphere. A_{ms}-A_{ion} and B_{ms}-B_{ion} represent the two red field lines in a steady-state magnetospheric configuration, the A_{ms}-A_{ion} line would move to B_{ms}-B_{ion} if the two lines rigidly rotate. However when dipolarization is involved when magnetospheric population rotates from A_{ms} to B_{ms}, the reconfigured magnetic field line (black) would connect the magnetospheric B_{ms} to B'_{ion} in the ionosphere instead of the original B_{ion}. Since the footpoint changes from A_{ion} to B'_{ion} when A_{ms} rotates to B_{ms}, the ionospheric counterpart therefore has a lower angular velocity than the magnetospheric counterpart. As a consequence, we would expect auroral intensification region to rotate at a lower angular velocity than its magnetospheric source, i.e., dipolarization. The divergence of footpoints (B_{ion} and B'_{ion}) in the ionosphere illustrated by the blue curve, which is produced by the formation of field-aligned currents and decrease of radial currents in the magnetosphere. We stress the importance of carefully comparing phenomena with different temporal scales. The transient phenomena often involve ongoing dynamics that change the connecting relations between the magnetosphere and ionosphere. By understanding the different angular velocities between these signatures, we could also potentially improve Saturn's magnetic model.

Although corotation of the dipolarized site could potentially well explain the recurrent nature of dipolarization and the associated subcorotating auroral region, corotation of the dipolarization might be in conflict with ion flows derived from Cassini's particle instruments that are well below rigid corotating velocity [*Mcandrews et al.*, 2009; *Thomsen et al.*, 2010, 2014]. We would like to point out that the subcorotations of magnetospheric sources (i.e., ENA emission and ion flow) are only average descriptions, while it remains mysterious why individual cases significantly vary. *Thomsen et al.* [2010] also show that different ion species (i.e., proton and water group) rotates at different angular velocities, which also vary with distance. It is then reasonable to assume a different angular velocity for electrons. In plasma environments, electrons are usually the most important current carriers and are also most likely frozen onto magnetic fields. Analysis of generalised Ohm's law with comprehensive measurements from magnetic field, plasma momentum and electric field is crucial to understand how ions and electrons are frozen onto magnetic fields [*Yao et al.*, 2017e].

3.2 PPO modulation on magnetospheric dynamics

Modulation from PPO was clearly identified at all three events presented in this study. Since the recurrent dipolarization event re-appearred after about one planetary rotation, therefore, each dipolarization shall be observed at a similar phase of PPO. It is unclear whether the dipolarization signature is caused by PPO's modulation.

PPO can not only produce periodic motion of Saturn's plasma sheet at nightside [*Arridge et al.*, 2011], but also cause periodic variations in the thickness of Saturn's nightside plasma sheet. However, there is no evidence that the modulation of plasma sheet motion or thickness can produce efficient particle acceleration, particularly for the 100s keV population. Even we assume that PPO could trigger reconnection and current disruption, however, this cannot explain why one planetary rotation later, the pre-condition are the same (Figure 2b for event 1). If PPO triggered a reconnection and current disruption at a certain modulation phase (e.g., *Jackman et al.* [2016b]), after one planetary rotation period, there is no reason to assume a same thin current sheet condition for current disruption and reconnection again. The blue curve in Figure 2b was unperturbed at the same phase of PPO, which also suggests that the later recurrent dipolarization is not purely a PPO modulation, otherwise there should be a similar decrease of B_r on the blue curve at the same phase of PPO. Internal processes (e.g., plasma instabilities) or external effects (e.g., the solar wind) may have influence in causing the observed recurrent B_r decrease.

If PPO produces dipolarization and the consequent aurora, then aurora should rotate with the same angular velocity as PPO (i.e., rigid rotation) but not only about 50% to 60% percent. If a source in the subcorotating magnetosphere causes the auroral intensification, then the auroral breakup region shall not rotate faster than the magnetosphere when considering the reconfiguration of magnetic field during auroral precipitation, which however is not supported by previous observations of ions and ENA. *Thomsen et al.* [2014] presented a statistical distribution of azimuthal ion velocity at different distance, and found that ion velocity remains roughly 100 km/s above 20 R_S, which correspond to $\sim$ 30% to 50% of planetary rigid corotation at 20 to 30 R_S. Either way, there exists fundamental conflict.

By checking the relative phases of the PPO for each event, and we were surprised to find that all the events were observed with North phases at around 90 deg, and South phases at around 300 deg, in which plasma and field lines are displaced inward and the current sheet would thick. Both effects are not favorable for reconnection, plasmoid or dipolarization to occur, which is opposite to the findings in *Jackman et al.* [2016a]. Clearly the events presented in this paper are not supported by PPO-modulation on reconnection (or dipolarization), while it remains unclear what controlled these processes. We would like to remind that we do not consider the inconsistency with PPO-phase is a strong conflict with the discovery in *Jackman et al.* [2016a], as we here report on dipolarization events while their research was about plasmoid. As we mentioned, the relations amongst dipolarization, reconnection and plasmoid could be extremely complicated.

Neither corotation of dipolarized region, nor PPO triggering dipolarization could fully explain the recurrent dipolarization phenomena reported in this paper. The two processes shall together involved, while it is unclear whether the two mechanisms could co-operate to produce such process. It requires further investigations on the two potential mechanisms, particularly with a combined view from other datasets, e.g, ENA and auroral emissions.

4 Summary

Magnetic dipolarization describes a reconfiguration of magnetic geometry from stretched magnetic field lines to more dipolar field lines. The change of magnetic field suggests a current system evolution, i.e., magnetospheric currents divert into the ionosphere, and is usually accompanied by precipitation of energetic electrons into the ionosphere and atmosphere. Therefore, magnetospheric dipolarization process is usually considered as an indicator of the magnetospheric dynamics for generating auroral intensifications in planetary polar regions. Although many pieces of evidence demonstrate the connections amongst these transient phenomena, we shall notice that details on their relations are far from understood.

Using measurements from multiple instruments onboard the Cassini spacecraft, we report recurrent type of dipolarization with three events. Our main results are summarised below.

(1) We reported three pairs of dipolarization events each reappeared by one planetary rotation period.

(2) We report dipolarization events (i.e., event 2) that exist at the dayside magnetosphere.

(3) Energetic electrons or ions are observed in all the three recurrent dipolarization events. In event 1 and 3, electrons were accelerated to 100s keV. In event 2 and 3, energetic ions were detected mostly at 10s keV, although 100 - 300 keV ions were also detected in event 2.

In our discussion, we compared two potential mechanisms (i.e., corotation and PPO modulation) in generating the recurrent dipolarization events, however each of them remains inconsistent with some previous measurements. What produced the recurrent dipolarization remains mysterious. Corotation of dipolarization site could well explain the reappear of energetic particles, while it is unclear why or how the site remain structured after one planetary rotation. The hypothesis of corotating dipolarization site also leads to a crisis to understand the well-known subcorotating plasma flows revealed by previous plasma dataset. This crisis does not exist in the other mechanism, i.e., the PPO modulation. However, PPO picture only provides a modulation of magnetic field outside of 10 R_S, while does not directly involve particle acceleration up to 30 R_S. Moreover, the relative phases of the PPO in all the three events correspond to thick and displaced inward plasma, which are not favorable for magnetic reconnection, plasmoid and dipolarization to occur.

Acknowledgments

ZY is a Marie-Curie COFUND postdoctoral fellow at the University of Liege. Co-funded by the European Union. A.J.C. is supported by STFC Consolidated Grants to UCL-MSSL (ST/K000977/1 and ST/N000722/1). A. R. is funded by the Belgian Fund for Scientific Research (FNRS). Z.Y., D.G., B.P. and J.C.G. acknowledge financial support from the Belgian Federal Science Policy Office (BELSPO) via the PRODEX Programme of ESA. Cassini operations are supported by NASA (managed by the Jet Propulsion Laboratory) and ESA. The data from Cassini's MAG, CAPS, MIMI and UVIS instruments onboard the NASA/ESA Cassini spacecraft are available in https://pds-ppi.igpp.ucla.edu/.

References

Akasofu, S.-I. (1964), The development of the auroral substorm, *Planetary and Space Science*, *12*(4), 273–282.

Allen, R., D. Mitchell, C. Paranicas, D. Hamilton, G. Clark, A. Rymer, S. Vines, E. Roelof, S. Krimigis, and J. Vandegriff (2018), Internal versus external sources of plasma at Saturn: Overview from MIMI/CHEMS data, *Journal of Geophysical Research: Space Physics*.

Andrews, D. J. (2011), Planetary-period oscillations in Saturn's magnetosphere, Ph.D. thesis, University of Leicester.

Andrews, D. J., S. Cowley, M. Dougherty, L. Lamy, G. Provan, and D. Southwood (2012), Planetary period oscillations in Saturn's magnetosphere: Evolution of magnetic oscillation properties from southern summer to post-equinox, *Journal of Geophysical Research: Space Physics*, *117*(A4).

Angelopoulos, V., J. P. McFadden, D. Larson, C. W. Carlson, S. B. Mende, H. Frey, T. Phan, D. G. Sibeck, K.-H. Glassmeier, U. Auster, et al. (2008), Tail reconnection triggering substorm onset, *Science*, *321*(5891), 931–935.

Arridge, C., C. Russell, K. Khurana, N. Achilleos, S. Cowley, M. Dougherty, D. Southwood, and E. Bunce (2008), Saturn's magnetodisc current sheet, *Journal of Geophysical Research: Space Physics*, *113*(A4).

Arridge, C. S., N. André, K. Khurana, C. Russell, S. Cowley, G. Provan, D. Andrews, C. Jackman, A. J. Coates, E. Sittler, et al. (2011), Periodic motion of Saturn's nightside plasma sheet, *Journal of Geophysical Research: Space Physics*, *116*(A11).

Arridge, C. S., J. P. Eastwood, C. M. Jackman, G.-K. Poh, J. A. Slavin, M. F. Thomsen, N. André, X. Jia, A. Kidder, L. Lamy, et al. (2016), Cassini in situ observations of long-duration magnetic reconnection in Saturn's magnetotail, *Nature Physics*, *12*(3), 268–271.

Badman, S., S. Cowley, J.-C. Gérard, and D. Grodent (2006), A statistical analysis of the location and width of Saturn's southern auroras, *Annales Geophysicae*, *24*(12), 3533–3545.

Balogh, A., M. Dougherty, R. Forsyth, D. Southwood, E. Smith, B. T. Tsurutani, N. Murphy, and M. Burton (1992), Magnetic field observations during the Ulysses flyby of Jupiter, *Science*, *257*(5076), 1515–1518.

Blanc, M., D. Andrews, A. Coates, D. Hamilton, C. Jackman, X. Jia, A. Kotova, M. Morooka, H. Smith, and J. Westlake (2015), Saturn plasma sources and associated transport processes, *Space Science Reviews*, *192*(1-4), 237–283.

Brandt, P., K. Khurana, D. Mitchell, N. Sergis, K. Dialynas, J. F. Carbary, E. Roelof, C. Paranicas, S. Krimigis, and B. Mauk (2010), Saturn's periodic magnetic field perturbations caused by a rotating partial ring current, *Geophysical Research Letters*, *37*(22).

Bunce, E., C. Arridge, J. Clarke, A. Coates, S. Cowley, M. K. Dougherty, J.-C. Gérard, D. Grodent, K. Hansen, J. Nichols, et al. (2008), Origin of Saturn's aurora: Simultaneous observations by Cassini and the Hubble Space Telescope, *Journal of Geophysical Research: Space Physics*, *113*(A9).

Bunce, E., S. Cowley, D. Talboys, M. Dougherty, L. Lamy, W. Kurth, P. Schippers, B. Cecconi, P. Zarka, C. S. Arridge, et al. (2010), Extraordinary field-aligned current signatures in Saturn's high-latitude magnetosphere: Analysis of Cassini data during Revolution 89, *Journal of Geophysical Research: Space Physics*, *115*(A10).

Carbary, J., and D. Mitchell (2014), Keogram analysis of ENA images at Saturn, *Journal of Geophysical Research: Space Physics*, *119*(3), 1771–1780.

Clarke, K., N. André, D. Andrews, A. Coates, S. Cowley, M. Dougherty, G. Lewis, H. McAndrews, J. Nichols, T. Robinson, et al. (2006), Cassini observations of planetary-period oscillations of Saturn's magnetopause, *Geophysical research letters*, *33*(23).

Cowley, S., D. Wright, E. Bunce, A. Carter, M. Dougherty, G. Giampieri, J. Nichols, and T. Robinson (2006), Cassini observations of planetary-period magnetic field oscillations in Saturn's magnetosphere: Doppler shifts and phase motion, *Geophysical research letters*, *33*(7).

Cowley, S., C. Arridge, E. Bunce, J. T. Clarke, A. Coates, M. K. Dougherty, J.-C. Gérard, D. Grodent, J. Nichols, and D. Talboys (2008), Auroral current systems in Saturn's magnetosphere: Comparison of theoretical models with Cassini and HST observations, in *Annales Geophysicae*, vol. 26, pp. 2613–2630, Copernicus Publications.

Delamere, P., A. Otto, X. Ma, F. Bagenal, and R. Wilson (2015), Magnetic flux circulation in the rotationally driven giant magnetospheres, *Journal of Geophysical Research: Space Physics*, *120*(6), 4229–4245.

Dialynas, K. (2018), Cassini/MIMI observations on the Dungey-Cycle reconnection and Kelvin-Helmholtz instability in Saturn's magnetosphere, *Journal of Geophysical Research: Space Physics*, doi:10.1029/2018JA025840.

Dialynas, K., P. Brandt, S. Krimigis, D. Mitchell, D. Hamilton, N. Krupp, and A. Rymer (2013), The extended Saturnian neutral cloud as revealed by global ENA simulations using Cassini/MIMI measurements, *Journal of Geophysical Research: Space Physics*, *118*(6), 3027–3041.

Dougherty, M., S. Kellock, D. Southwood, A. Balogh, E. Smith, B. Tsurutani, B. Gerlach, K.-H. Glassmeier, F. Gleim, C. Russell, et al. (2004), The Cassini magnetic field investigation, in *The Cassini-Huygens Mission*, pp. 331–383, Springer.

Espinosa, S. A., and M. K. Dougherty (2000), Periodic perturbations in Saturn's magnetic field, *Geophysical research letters*, *27*(17), 2785–2788.

Espinosa, S. A., D. J. Southwood, and M. K. Dougherty (2003), How can Saturn impose its rotation period in a noncorotating magnetosphere?, *Journal of Geophysical Research: Space Physics*, *108*(A2).

Esposito, L. W., C. A. Barth, J. E. Colwell, G. M. Lawrence, W. E. McClintock, A. I. F. Stewart, H. U. Keller, A. Korth, H. Lauche, M. C. Festou, et al. (2004), The Cassini ultraviolet imaging spectrograph investigation, in *The Cassini-Huygens Mission*, pp. 299–361, Springer.

Grodent, D., J.-C. Gérard, S. Cowley, E. Bunce, and J. Clarke (2005), Variable morphology of Saturn's southern ultraviolet aurora, *Journal of Geophysical Research: Space Physics*, *110*(A7).

Guo, R. L., Z. H. Yao, Y. Wei, L. C. Ray, I. J. Rae, C. Arridge, A. Coates, P. Delamere, N. Sergis, P. Kollmann, et al. (2018), Rotationally driven magnetic reconnection in Rotationally driven magnetic reconnection in Saturn's dayside, *Nature Astronomy*, doi: 10.1038/s41550-018-0461-9.

Henderson, M. G. (2009), Observational evidence for an inside-out substorm onset scenario, *Ann. Geophys*, *27*(5), 2129–2140.

Hesse, M., and J. Birn (1991), On dipolarization and its relation to the substorm current wedge, *Journal of Geophysical Research: Space Physics*, *96*(A11), 19,417–19,426.

Hones, E. W. (1963), Motions of charged particles trapped in the earth's magnetosphere, *Journal of Geophysical Research*, *68*(5), 1209–1219.

Hunt, G., S. Cowley, G. Provan, E. Bunce, I. Alexeev, E. Belenkaya, V. Kalegaev, M. Dougherty, and A. Coates (2015), Field-aligned currents in Saturn's northern nightside magnetosphere: Evidence for interhemispheric current flow associated with planetary period oscillations, *Journal of Geophysical Research: Space Physics*, *120*(9), 7552–7584.

Jackman, C., C. Russell, D. Southwood, C. Arridge, N. Achilleos, and M. Dougherty (2007), Strong rapid dipolarizations in Saturn's magnetotail: In situ evidence of reconnection, *Geophysical research letters*, *34*(11).

Jackman, C., J. Slavin, and S. Cowley (2011), Cassini observations of plasmoid structure and dynamics: Implications for the role of magnetic reconnection in magnetospheric circulation at Saturn, *Journal of Geophysical Research: Space Physics*, *116*(A10).

Jackman, C., M. Thomsen, D. Mitchell, N. Sergis, C. Arridge, M. Felici, S. Badman, C. Paranicas, X. Jia, G. Hospodarksy, et al. (2015), Field dipolarization in Saturn's magnetotail with planetward ion flows and energetic particle flow bursts: Evidence of quasi-steady reconnection, *Journal of Geophysical Research: Space Physics*, *120*(5), 3603–3617.

Jackman, C., G. Provan, and S. W. H. Cowley (2016a), Reconnection events in Saturn's magnetotail: Dependence of plasmoid occurrence on planetary period oscillation phase, *Journal of Geophysical Research: Space Physics*, *121*(4), 2922–2934.

Jackman, C. M., N. Achilleos, S. W. Cowley, E. J. Bunce, A. Radioti, D. Grodent, S. V. Badman, M. K. Dougherty, and W. Pryor (2013), Auroral counterpart of magnetic field dipolarizations in Saturn's tail, *Planetary and Space Science*, *82*, 34–42.

Jackman, C. M., G. Provan, and S. W. H. Cowley (2016b), Reconnection events in Saturn's magnetotail: Dependence of plasmoid occurrence on planetary period oscillation phase, *Journal of Geophysical Research: Space Physics*, *121*(4), 2922–2934, doi: 10.1002/2015ja021985.

Keiling, A., V. Angelopoulos, A. Runov, J. Weygand, S. Apatenkov, S. Mende, J. McFadden, D. Larson, O. Amm, K.-H. Glassmeier, et al. (2009), Substorm current wedge driven by plasma flow vortices: THEMIS observations, *Journal of Geophysical Research: Space Physics (1978–2012)*, *114*(A1).

Kivelson, M. G. (2005), The current systems of the Jovian magnetosphere and ionosphere and predictions for Saturn, *The Outer Planets and their Moons*, pp. 299–318.

Krimigis, S., D. Mitchell, D. Hamilton, S. Livi, J. Dandouras, S. Jaskulek, T. Armstrong, J. Boldt, A. Cheng, G. Gloeckler, et al. (2004), Magnetosphere imaging instrument (MIMI) on the Cassini mission to Saturn/Titan, *Space Science Reviews*, *114*(1), 233–329.

Krimigis, S., N. Sergis, D. Mitchell, D. Hamilton, and N. Krupp (2007), A dynamic, rotating ring current around Saturn, *Nature*, *450*(7172), 1050–1053.

Kronberg, E., J. Woch, N. Krupp, A. Lagg, K. Khurana, and K.-H. Glassmeier (2005), Mass release at Jupiter: Substorm-like processes in the Jovian magnetotail, *Journal of Geophysical Research: Space Physics (1978–2012)*, *110*(A3).

Lui, A. (1996), Current disruption in the Earth's magnetosphere: Observations and models, *Journal of Geophysical Research: Space Physics (1978–2012)*, *101*(A6), 13,067–13,088.

Lui, A., P. Yoon, C. Mok, and C.-M. Ryu (2008), Inverse cascade feature in current disruption, *Journal of Geophysical Research: Space Physics*, *113*(A1).

Masters, A., M. Thomsen, S. Badman, C. S. Arridge, D. Young, A. J. Coates, and M. Dougherty (2011), Supercorotating return flow from reconnection in Saturn's magnetotail, *Geophysical Research Letters*, *38*(3).

Mauk, B., J. Saur, D. Mitchell, E. Roelof, P. Brandt, T. Armstrong, D. Hamilton, S. Krimigis, N. Krupp, S. Livi, et al. (2005), Energetic particle injections in Saturn's magnetosphere, *Geophysical research letters*, *32*(14).

Mcandrews, H. J., M. F. Thomsen, C. S. Arridge, C. Jackman, R. Wilson, M. Henderson, R. Tokar, K. K. Khurana, E. C. Sittler, A. J. Coates, et al. (2009), Plasma in Saturn's nightside magnetosphere and the implications for global circulation, *Planetary and Space Science*, *57*(14-15), 1714–1722.

McPherron, R., C. Russell, M. Kivelson, and P. Coleman (1973), Substorms in space: The correlation between ground and satellite observations of the magnetic field, *Radio Science*, *8*(11), 1059–1076.

Mitchell, D., P. Brandt, E. Roelof, J. Dandouras, S. Krimigis, and B. Mauk (2005), Energetic neutral atom emissions from Titan interaction with Saturn's magnetosphere, *Science*, *308*(5724), 989–992.

Mitchell, D., S. Krimigis, C. Paranicas, P. Brandt, J. Carbary, E. Roelof, W. Kurth, D. Gurnett, J. Clarke, J. Nichols, et al. (2009a), Recurrent energization of plasma in the midnight-to-dawn quadrant of Saturn's magnetosphere, and its relationship to auroral UV and radio emissions, *Planetary and Space Science*, *57*(14), 1732–1742.

Mitchell, D., W. Kurth, G. Hospodarsky, N. Krupp, J. Saur, B. Mauk, J. Carbary, S. Krimigis, M. Dougherty, and D. Hamilton (2009b), Ion conics and electron beams associated with auroral processes on Saturn, *Journal of Geophysical Research: Space Physics*, *114*(A2).

Mitchell, D., J. Carbary, E. Bunce, A. Radioti, S. Badman, W. Pryor, G. Hospodarsky, and W. Kurth (2016), Recurrent pulsations in Saturn's high latitude magnetosphere, *Icarus*, *263*, 94–100.

Nichols, J. D., S. V Badman, K. Baines, R. Brown, E. Bunce, J. Clarke, S. Cowley, F. Crary, M. Dougherty, J.-C. Gérard, et al. (2014), Dynamic auroral storms on Saturn as observed by the Hubble Space Telescope, *Geophysical research letters*, *41*(10), 3323–3330.

Palmaerts, B., E. Roussos, N. Krupp, W. Kurth, D. Mitchell, and J. Yates (2016), Statistical analysis and multi-instrument overview of the quasi-periodic 1-hour pulsations in Saturn's outer magnetosphere, *Icarus*, *271*, 1–18, doi:10.1016/j.icarus.2016.01.025.

Pilkington, N., N. Achilleos, C. Arridge, P. Guio, A. Masters, L. Ray, N. Sergis, M. Thomsen, A. Coates, and M. Dougherty (2015), Asymmetries observed in Saturn's magnetopause geometry, *Geophysical research letters*, *42*(17), 6890–6898.

Provan, G., D. J. Andrews, C. S. Arridge, A. J. Coates, S. Cowley, G. Cox, M. Dougherty, and C. Jackman (2012), Dual periodicities in planetary-period magnetic field oscillations in Saturn's tail, *Journal of Geophysical Research: Space Physics*, *117*(A1).

Provan, G., S. Cowley, T. Bradley, E. Bunce, G. Hunt, and M. Dougherty (2018), Planetary Period Oscillations in Saturn's Magnetosphere: Cassini Magnetic Field Observations Over the Northern Summer Solstice Interval, *Journal of Geophysical Research: Space Physics*.

Radioti, A., D. Grodent, J.-C. Gérard, S. E. Milan, R. C. Fear, C. Jackman, B. Bonfond, and W. Pryor (2014), Saturn's elusive nightside polar arc, *Geophysical Research Letters*, *41*(18), 6321–6328.

Radioti, A., D. Grodent, J.-C. Gérard, E. Roussos, D. Mitchell, B. Bonfond, and W. Pryor (2015), Auroral spirals at Saturn, *Journal of Geophysical Research: Space Physics*, *120*(10), 8633–8643.

Radioti, A., D. Grodent, X. Jia, J.-C. Gérard, B. Bonfond, W. Pryor, J. Gustin, D. Mitchell, and C. Jackman (2016), A multi-scale magnetotail reconnection event at Saturn and associated flows: Cassini/UVIS observations, *Icarus*, *263*, 75–82.

Roussos, E., N. Krupp, D. Mitchell, C. Paranicas, S. Krimigis, M. Andriopoulou, B. Palmaerts, W. Kurth, S. Badman, A. Masters, et al. (2016), Quasi-periodic injections of relativistic electrons in Saturn's outer magnetosphere, *Icarus*, *263*, 101–116.

Runov, A., S. Kiehas, and S. Li (2017), Dawn-Dusk Asymmetries in Magnetotail Transients, *Dawn-Dusk Asymmetries in Planetary Plasma Environments*, *230*, 233.

Saur, J., B. Mauk, D. Mitchell, N. Krupp, K. Khurana, S. Livi, S. Krimigis, P. Newell, D. Williams, P. Brandt, et al. (2006), Anti-planetward auroral electron beams at Saturn, *Nature*, *439*(7077), 699–702.

Schippers, P., N. André, D. Gurnett, G. R. Lewis, A. Persoon, and A. J. Coates (2012), Identification of electron field-aligned current systems in Saturn's magnetosphere, *Journal of Geophysical Research: Space Physics*, *117*(A5).

Slavin, J. A., B. J. Anderson, D. N. Baker, M. Benna, S. A. Boardsen, G. Gloeckler, R. E. Gold, G. C. Ho, H. Korth, S. M. Krimigis, et al. (2010), MESSENGER observations of extreme loading and unloading of Mercurys magnetic tail, *Science*, *329*(5992), 665–668.

Smith, A., C. Jackman, M. Thomsen, N. Sergis, D. Mitchell, and E. Roussos (2018), Dipolarization Fronts with Associated Energized Electrons in Saturn's Magnetotail, *Journal of Geophysical Research: Space Physics*.

Stallard, T., S. Miller, M. Lystrup, N. Achilleos, E. J. Bunce, C. S. Arridge, M. K. Dougherty, S. W. Cowley, S. V. Badman, D. L. Talboys, et al. (2008), Complex structure within Saturn's infrared aurora, *Nature*, *456*(7219), 214–217.

Talboys, D., C. Arridge, E. Bunce, A. Coates, S. Cowley, M. Dougherty, and K. Khurana (2009), Signatures of field-aligned currents in Saturn's nightside magnetosphere, *Geophysical Research Letters*, *36*(19).

Thomsen, M., D. Reisenfeld, D. Delapp, R. Tokar, D. Young, F. Crary, E. Sittler, M. McGraw, and J. Williams (2010), Survey of ion plasma parameters in Saturn's magnetosphere, *Journal of Geophysical Research: Space Physics*, *115*(A10).

Thomsen, M., C. Jackman, R. Tokar, and R. Wilson (2014), Plasma flows in Saturn's nightside magnetosphere, *Journal of Geophysical Research: Space Physics*, *119*(6), 4521–4535.

Thomsen, M., C. Jackman, S. W. H. Cowley, X. Jia, M. Kivelson, and G. Provan (2017), Evidence for periodic variations in the thickness of Saturn's nightside plasma sheet, *Journal of Geophysical Research: Space Physics*, *122*(1), 280–292.

Vasyliunas, V. (1983), Plasma distribution and flow, *Physics of the Jovian magnetosphere*, *1*, 395–453.

Waite, J. H., M. R. Combi, W.-H. Ip, T. E. Cravens, R. L. McNutt, W. Kasprzak, R. Yelle, J. Luhmann, H. Niemann, D. Gell, et al. (2006), Cassini ion and neutral mass spectrometer: Enceladus plume composition and structure, *science*, *311*(5766), 1419–1422.

Yao, Z. (2017), Observations of loading-unloading process at Saturn distant magnetotail, *Earth and Planetary Physics*, *1*, 53–57.

Yao, Z., Z. Pu, S. Fu, V. Angelopoulos, M. Kubyshkina, X. Xing, L. Lyons, Y. Nishimura, L. Xie, X. Wang, et al. (2012), Mechanism of substorm current wedge formation: THEMIS observations, *Geophysical Research Letters*, *39*(13).

Yao, Z., W. Sun, S. Fu, Z. Pu, J. Liu, V. Angelopoulos, X.-J. Zhang, X. Chu, Q. Shi, R. Guo, et al. (2013), Current structures associated with dipolarization fronts, *Journal of Geophysical Research: Space Physics*, *118*(11), 6980–6985.

Yao, Z., A. Coates, L. Ray, I. Rae, D. Grodent, G. H. Jones, M. Dougherty, C. Owen, R. Guo, W. Dunn, et al. (2017a), Corotating magnetic reconnection site in Saturn's magnetosphere, *The Astrophysical Journal Letters*, *846*(2), L25.

Yao, Z., D. Grodent, L. Ray, I. Rae, A. Coates, Z. Pu, A. Lui, A. Radioti, J. Waite, G. Jones, et al. (2017b), Two fundamentally different drivers of dipolarizations at Saturn, *Journal of Geophysical Research: Space Physics*, doi:10.1002/2017JA024060.

Yao, Z., A. Radioti, I. Rae, J. Liu, D. Grodent, L. Ray, S. Badman, A. Coates, J.-C. Gérard, J. Waite, et al. (2017c), Mechanisms of Saturn's Near-Noon Transient Aurora: In Situ Evidence From Cassini Measurements, *Geophysical Research Letters*, *44*(22), 217–228, doi:10.1002/2017GL075108.

Yao, Z., I. Rae, A. Lui, K. Murphy, C. Owen, Z. Pu, C. Forsyth, D. Grodent, Q.-G. Zong, A. Du, et al. (2017d), An explanation of auroral intensification during the substorm expansion phase, *Journal of Geophysical Research: Space Physics*, *122*, 8560–8576.

Yao, Z., I. Rae, R. Guo, A. Fazakerley, C. Owen, R. Nakamura, W. Baumjohann, C. E. Watt, K. Hwang, B. Giles, et al. (2017e), A direct examination of the dynamics of dipolarization fronts using MMS, *Journal of Geophysical Research: Space Physics*, *122*(4), 4335–4347.

Young, D., J. Berthelier, M. Blanc, J. Burch, A. Coates, R. Goldstein, M. Grande, T. Hill, R. Johnson, V. Kelha, et al. (2004), Cassini plasma spectrometer investigation, in *The Cassini-Huygens Mission*, pp. 1–112, Springer.

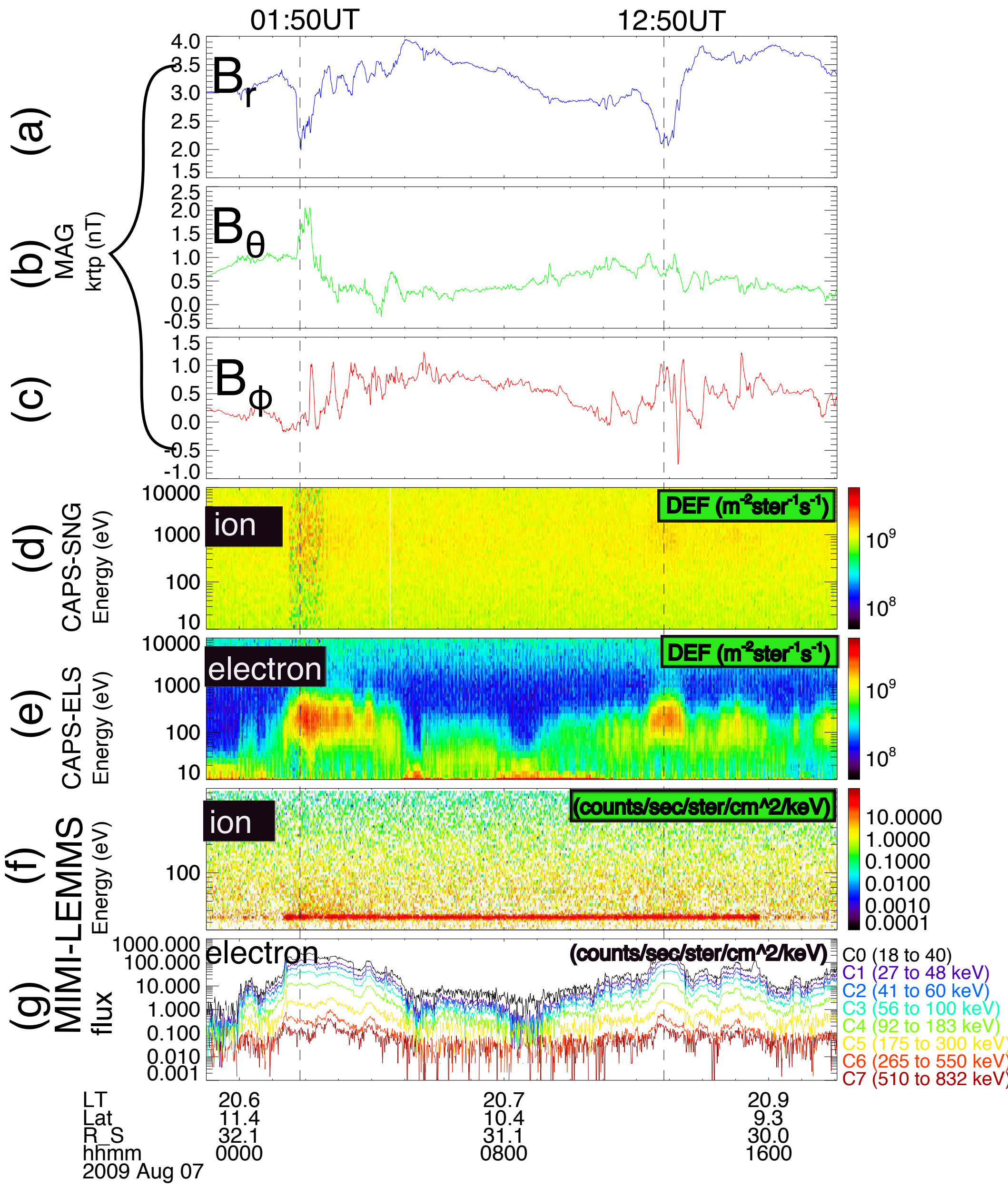

814 **Figure 1.** Overview of magnetic fields and plasma measurements on August 07, 2009. Two dipolarization processes are marked by the vertical dashed black lines. (a-c) the magnetic fields are in KRTP coordinates. (d) ion differential energy flux from CAPS-SNG. (e) electron differential energy flux from CAPS-ELS. (f) energetic ion counts from MIMI-LEMMS. (g) energetic electron counts from MIMI-LEMMS detector.

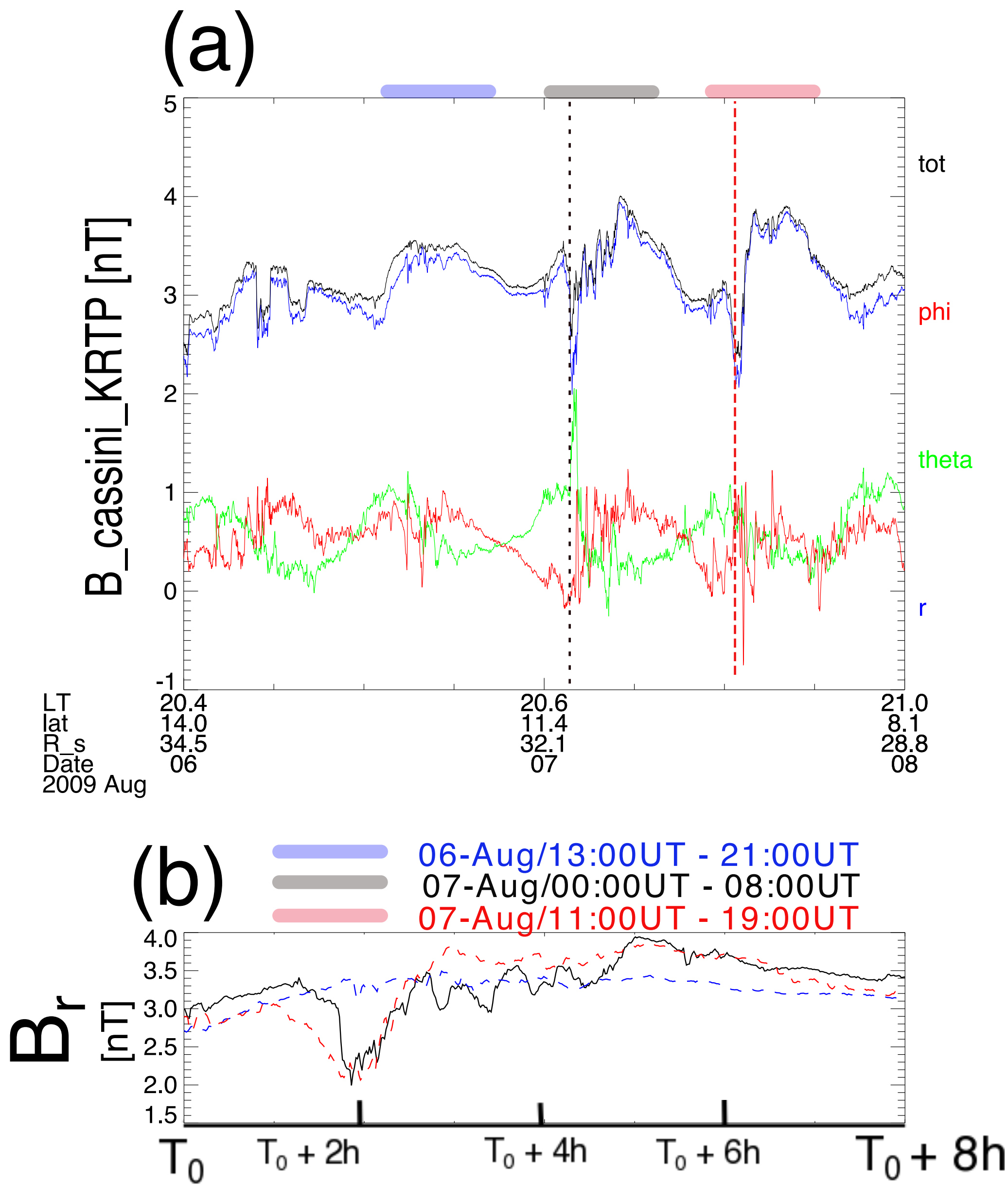

818 **Figure 2.** Comparison of the background (blue), DP1 (black) and DP2 (red) events. (a) Overview of the
819 one-minute resolution magnetic field between 06 August and 08 August, and (b) superimposed plots of
820 magnetic fields for the selected three periods.

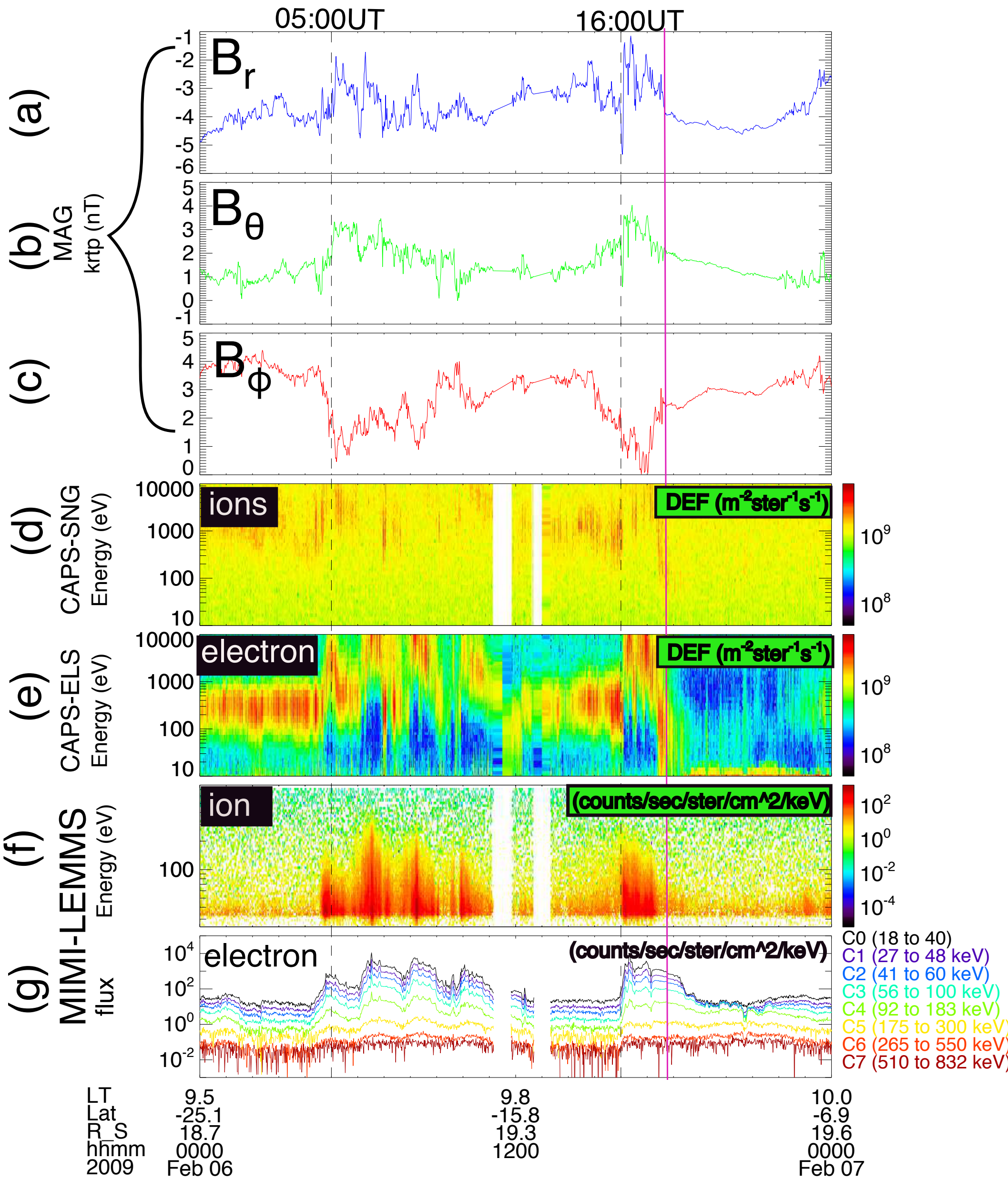

821 **Figure 3.** Overview of magnetic fields and plasma measurements on February 06, 2009. The format is the
822 same as Figure 1.

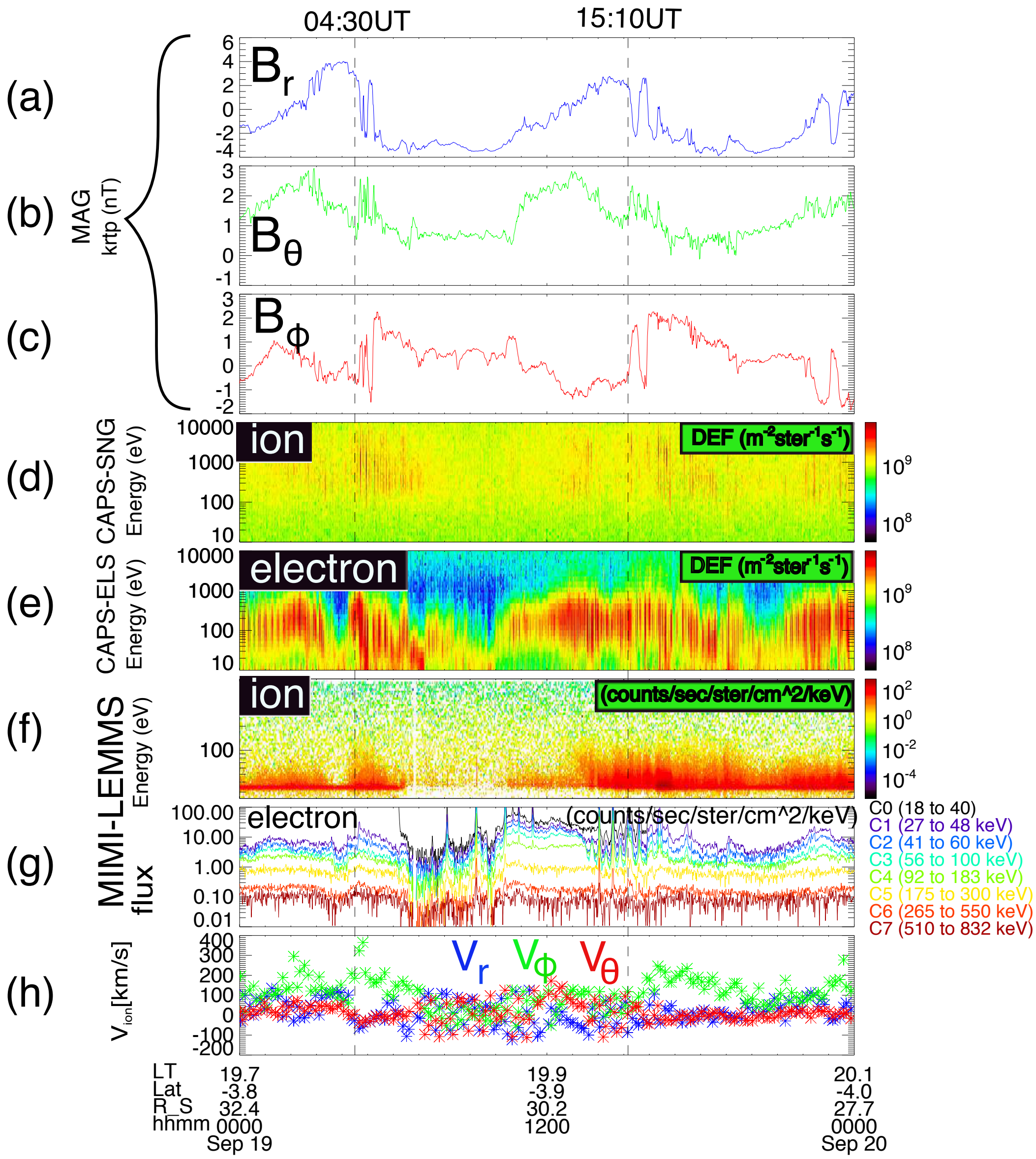

Figure 4. Overview of magnetic fields and plasma measurements on September 19, 2010. The format of Figure 4(a-g) is the same as Figure 1. Figure 4h shows the derived ion velocity by numerical integration of CAPS Ion Mass Spectrometer mesurements.

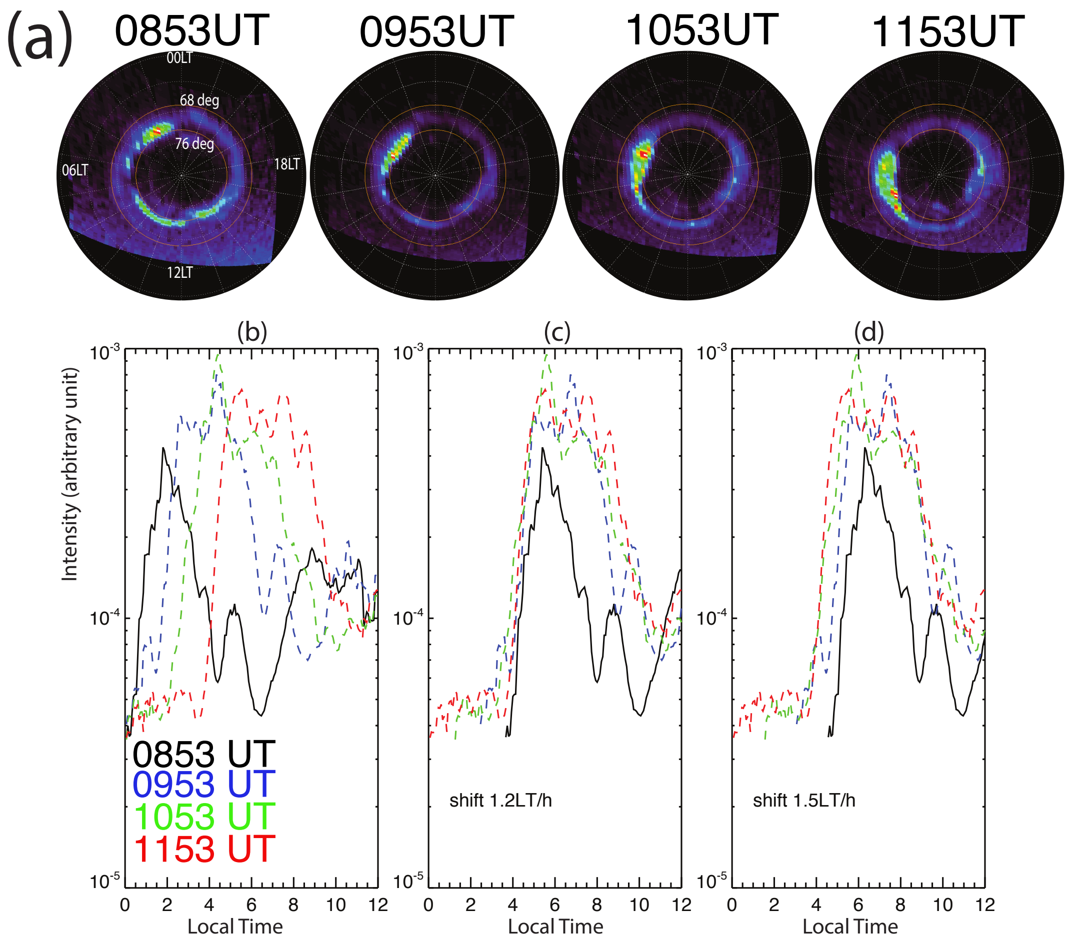

826 **Figure 5.** (a) A sequence of aurora images from 08:53 UT to 11:53 UT (separated by one hour between
827 each two) on DOY 129, 2008. (b) Local time distribution of integrated auroral intensity between 68 and 76
828 deg latitudes for the four images in Figure 3a. (c, d) The profiles of 08:53 UT, 09:53 UT and 10:53 UT are
829 shifted to 11:53 UT by adding a local time rate of 1.2 LT/h and 1.5 LT/h.

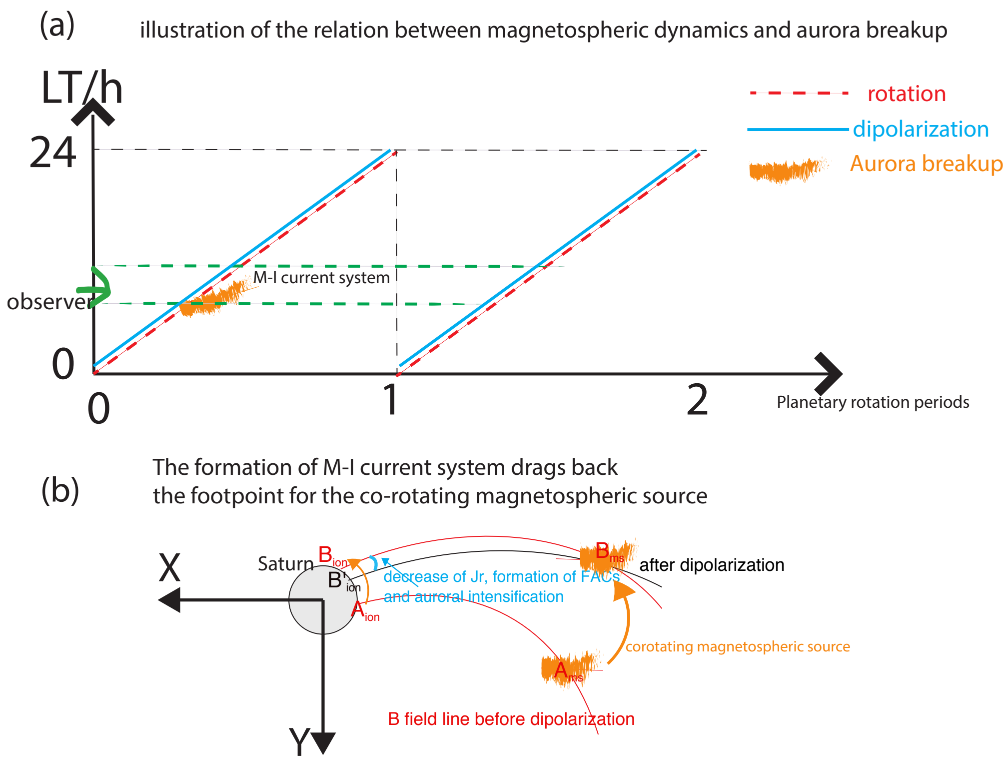

Figure 6. Illustration of relations between aurora breakup and magnetospheric sources. (a) how local time of dipolarization and aurora change with time. The red dashed line indicates rigid planetary rotation, the solid blue line shows local time of dipolarization site changes with time, and the orange cloud indicates the local time of enhanced aurora site changing with time.(b) how the footpoint of magnetospheric source changes during the development of auroral current system, in the view from the north pole of Saturn. The two red curves (A_{ms}-A_{ion} and B_{ms}-B_{ion}) represent two field lines in a steady-state magnetospheric configuration, the A_{ms}-A_{ion} field line would naturally rotates to B_{ms}-B_{ion} if there is no reconfiguration of magnetic field. During auroral intensification period, the magnetic field B_{ms}-B_{ion} would evolve into the black curve (B_{ms}-B'_{ion}) during and after dipolarization due to the formation of the magnetosphere-ionosphere current system. During this process, the footpoint of a corotating magnetospheric source would subcorotate with the planet, due to the changing geometry of magnetic field lines that connect the magnetosphere and ionosphere. Therefore, the footpoint would have a lower angular velocity than the magnetospheric counterpart.

Figure 1.

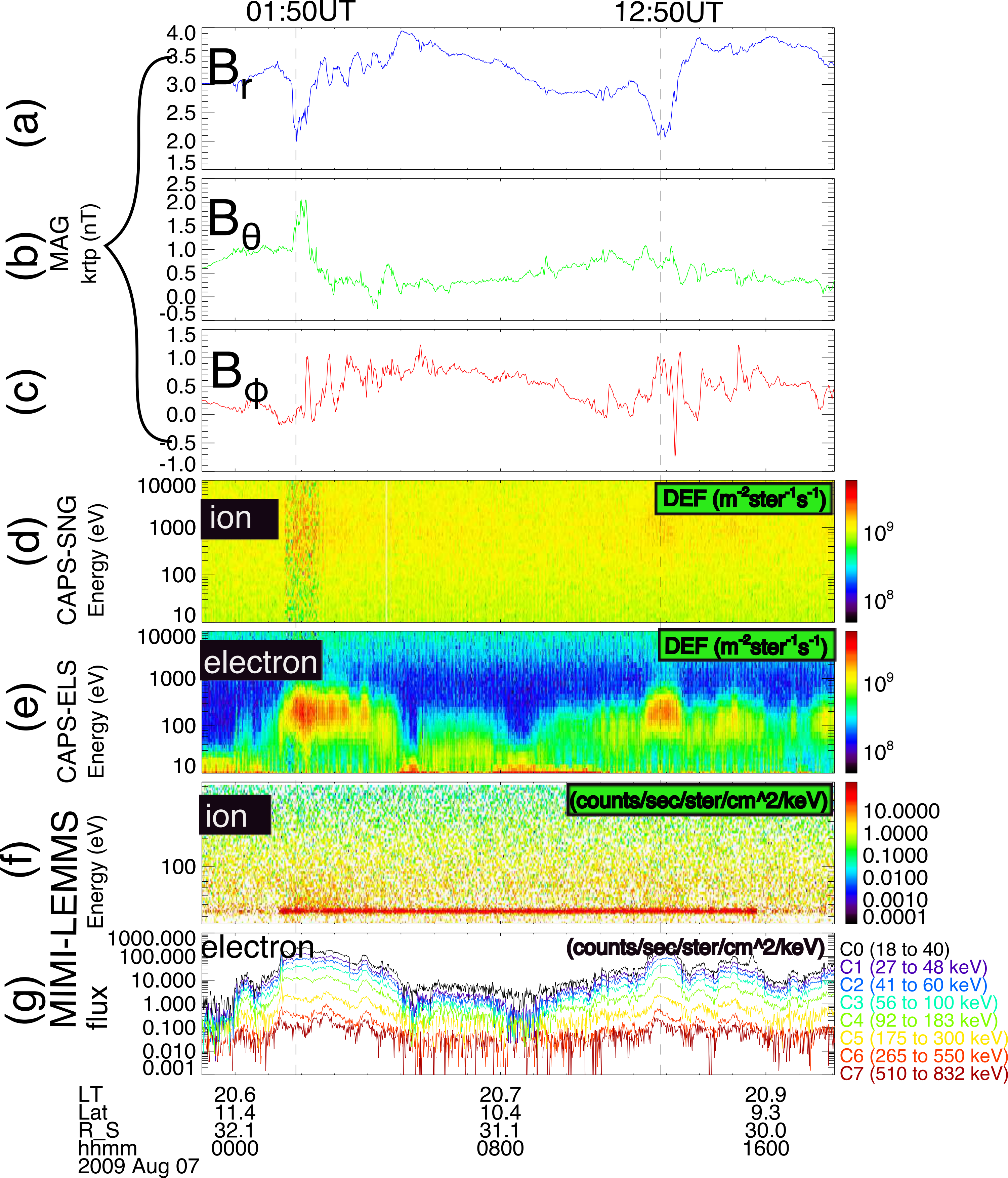

01:50UT
12:50UT
(a)
(b)
(c)
(d)
(e)
(f)
(g)
MAG krtp (nT)
Br
Bθ
Bφ
CAPS-SNG Energy (eV)
ion
DEF (m^-2ster^-1s^-1)
CAPS-ELS Energy (eV)
electron
DEF (m^-2ster^-1s^-1)
MIMI-LEMMS Energy (eV)
ion
(counts/sec/ster/cm^2/keV)
MIMI-LEMMS flux
electron
(counts/sec/ster/cm^2/keV)
C0 (18 to 40)
C1 (27 to 48 keV)
C2 (41 to 60 keV)
C3 (56 to 100 keV)
C4 (92 to 183 keV)
C5 (175 to 300 keV)
C6 (265 to 550 keV)
C7 (510 to 832 keV)
LT 20.6 20.7 20.9
Lat 11.4 10.4 9.3
R_S 32.1 31.1 30.0
hhmm 0000 0800 1600
2009 Aug 07

Figure 2.

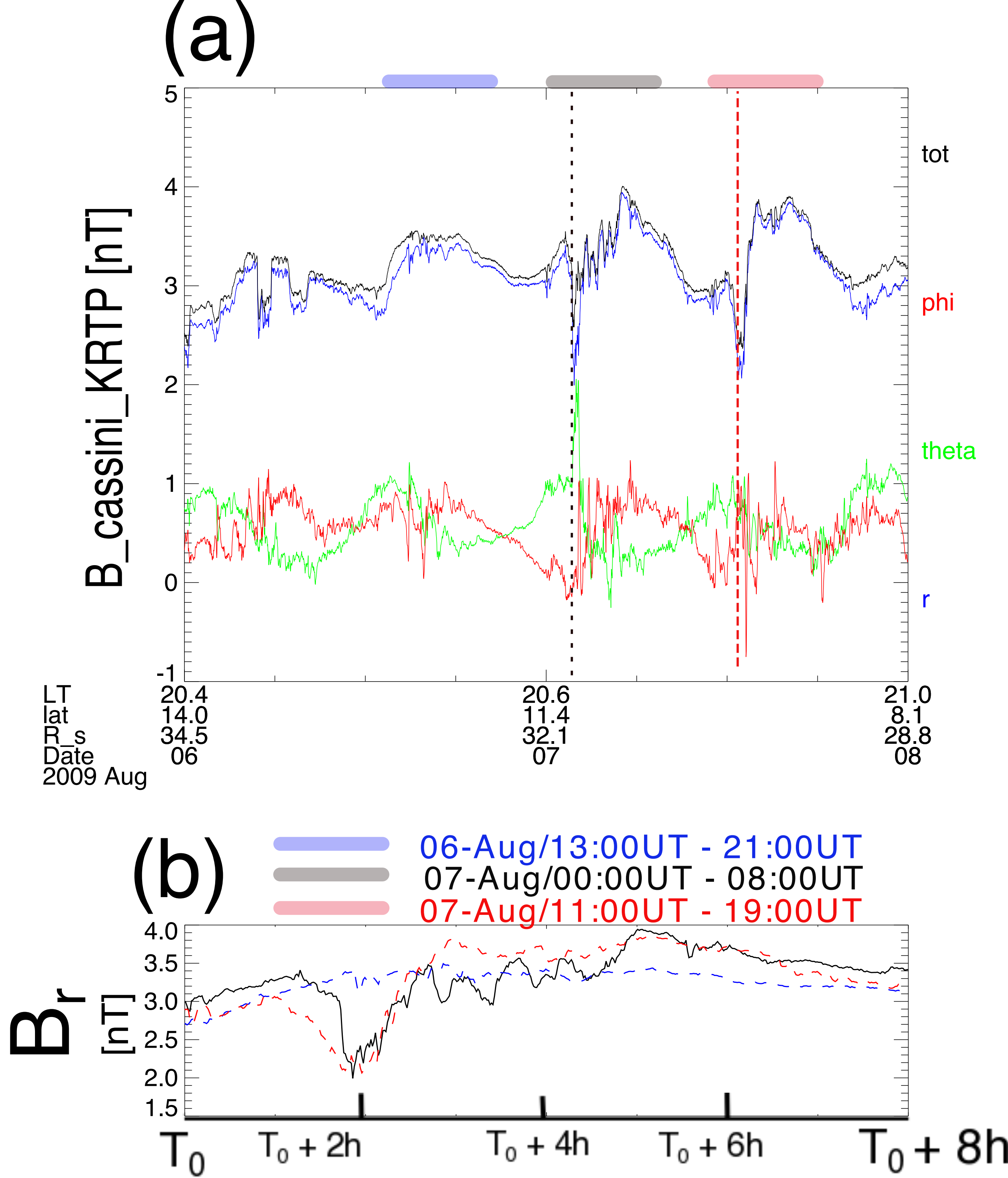
(a)
B_cassini_KRTP [nT]
tot
phi
theta
r
LT
lat
R_s
Date
2009 Aug
20.4
14.0
34.5
06
20.6
11.4
32.1
07
21.0
8.1
28.8
08
(b)
06-Aug/13:00UT - 21:00UT
07-Aug/00:00UT - 08:00UT
07-Aug/11:00UT - 19:00UT
B_r [nT]
T_0
$T_0 + 2h$
$T_0 + 4h$
$T_0 + 6h$
$T_0 + 8h$

Figure 3.

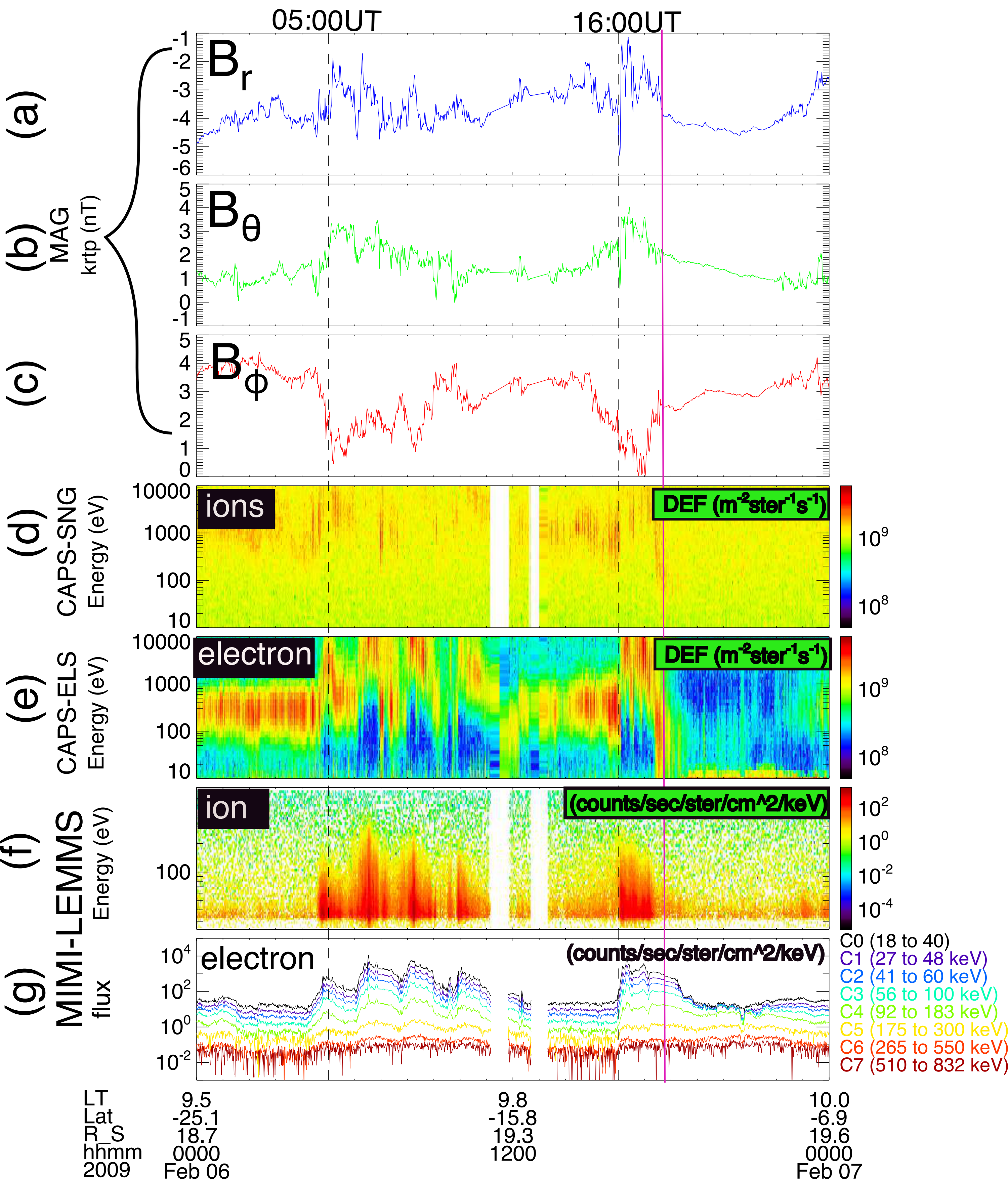

05:00UT
16:00UT
(a)
(b)
(c)
MAG
krtp (nT)
B_r
B_θ
B_ϕ
(d)
CAPS-SNG
Energy (eV)
ions
DEF (m^{-2}ster^{-1}s^{-1})
(e)
CAPS-ELS
Energy (eV)
electron
DEF (m^{-2}ster^{-1}s^{-1})
(f)
MIMI-LEMMS
Energy (eV)
ion
(counts/sec/ster/cm^2/keV)
(g)
flux
electron
(counts/sec/ster/cm^2/keV)
C0 (18 to 40)
C1 (27 to 48 keV)
C2 (41 to 60 keV)
C3 (56 to 100 keV)
C4 (92 to 183 keV)
C5 (175 to 300 keV)
C6 (265 to 550 keV)
C7 (510 to 832 keV)
LT 9.5 9.8 10.0
Lat -25.1 -15.8 -6.9
R_S 18.7 19.3 19.6
hhmm 0000 1200 0000
2009 Feb 06 Feb 07

Figure 4.

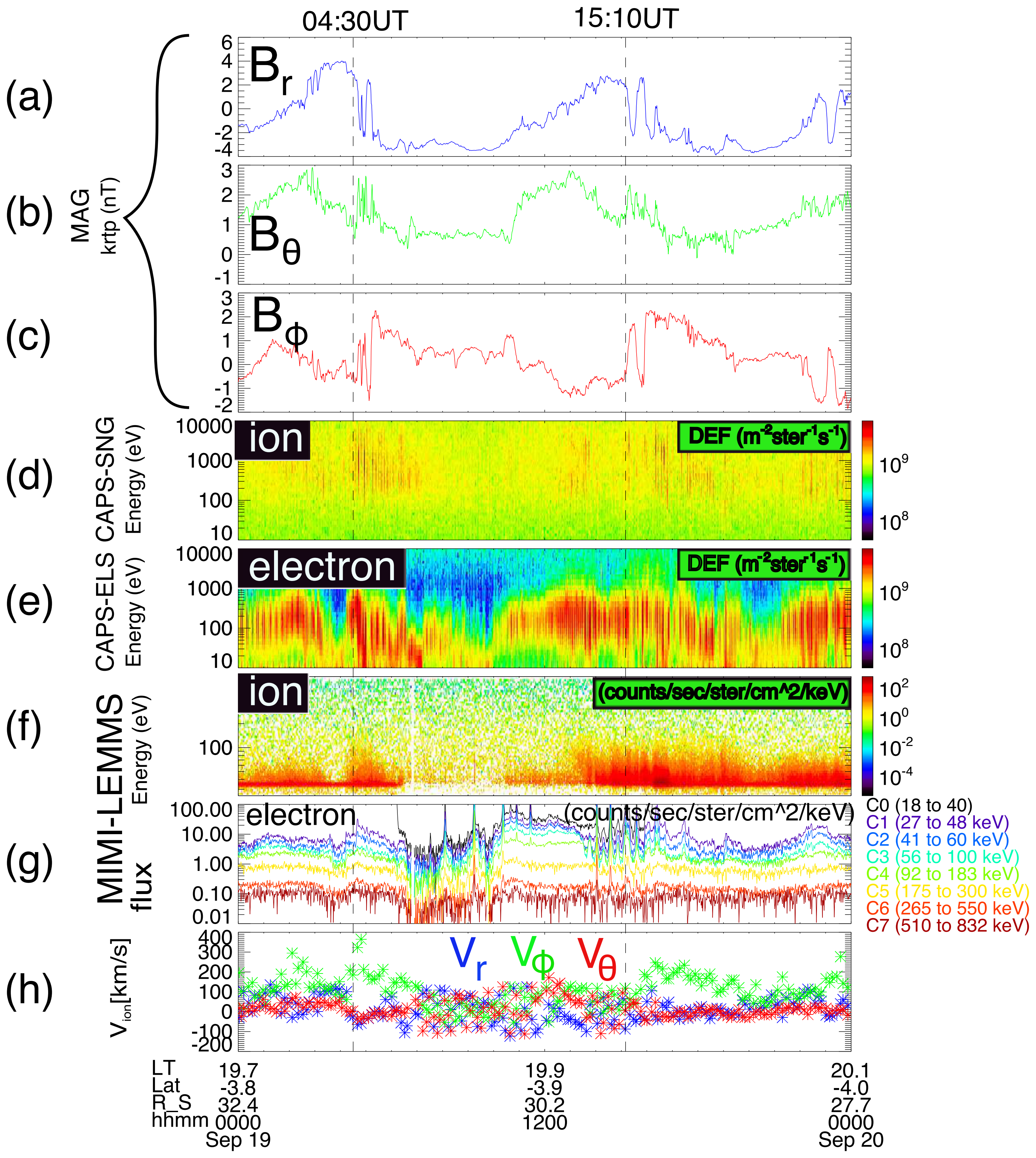
04:30UT
15:10UT
(a)
(b)
(c)
(d)
(e)
(f)
(g)
(h)
MAG
krtp (nT)
Br
Bθ
Bφ
CAPS-SNG
Energy (eV)
ion
DEF (m-2ster-1s-1)
CAPS-ELS
Energy (eV)
electron
DEF (m-2ster-1s-1)
MIMI-LEMMS
Energy (eV)
ion
(counts/sec/ster/cm^2/keV)
flux
electron
(counts/sec/ster/cm^2/keV)
C0 (18 to 40)
C1 (27 to 48 keV)
C2 (41 to 60 keV)
C3 (56 to 100 keV)
C4 (92 to 183 keV)
C5 (175 to 300 keV)
C6 (265 to 550 keV)
C7 (510 to 832 keV)
Vion[km/s]
Vr
Vφ
Vθ
LT 19.7 19.9 20.1
Lat -3.8 -3.9 -4.0
R_S 32.4 30.2 27.7
hhmm 0000 1200 0000
Sep 19
Sep 20

Figure 5.

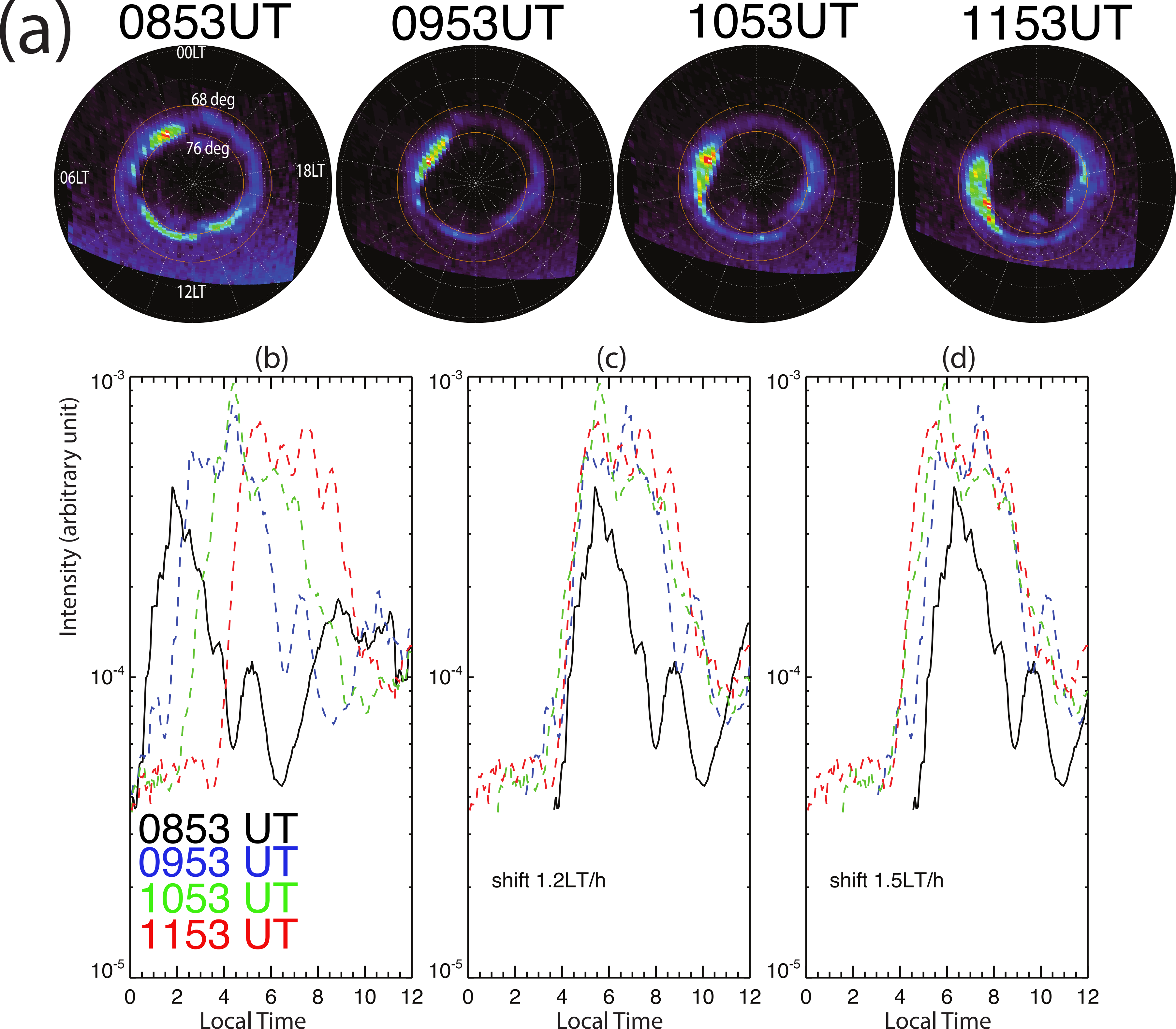
(a)
0853UT
0953UT
1053UT
1153UT
00LT
68 deg
76 deg
06LT
18LT
12LT
(b)
(c)
(d)
Intensity (arbitrary unit)
10^-3
10^-4
10^-5
0853 UT
0953 UT
1053 UT
1153 UT
shift 1.2LT/h
shift 1.5LT/h
0
2
4
6
8
10
12
Local Time

Figure 6.

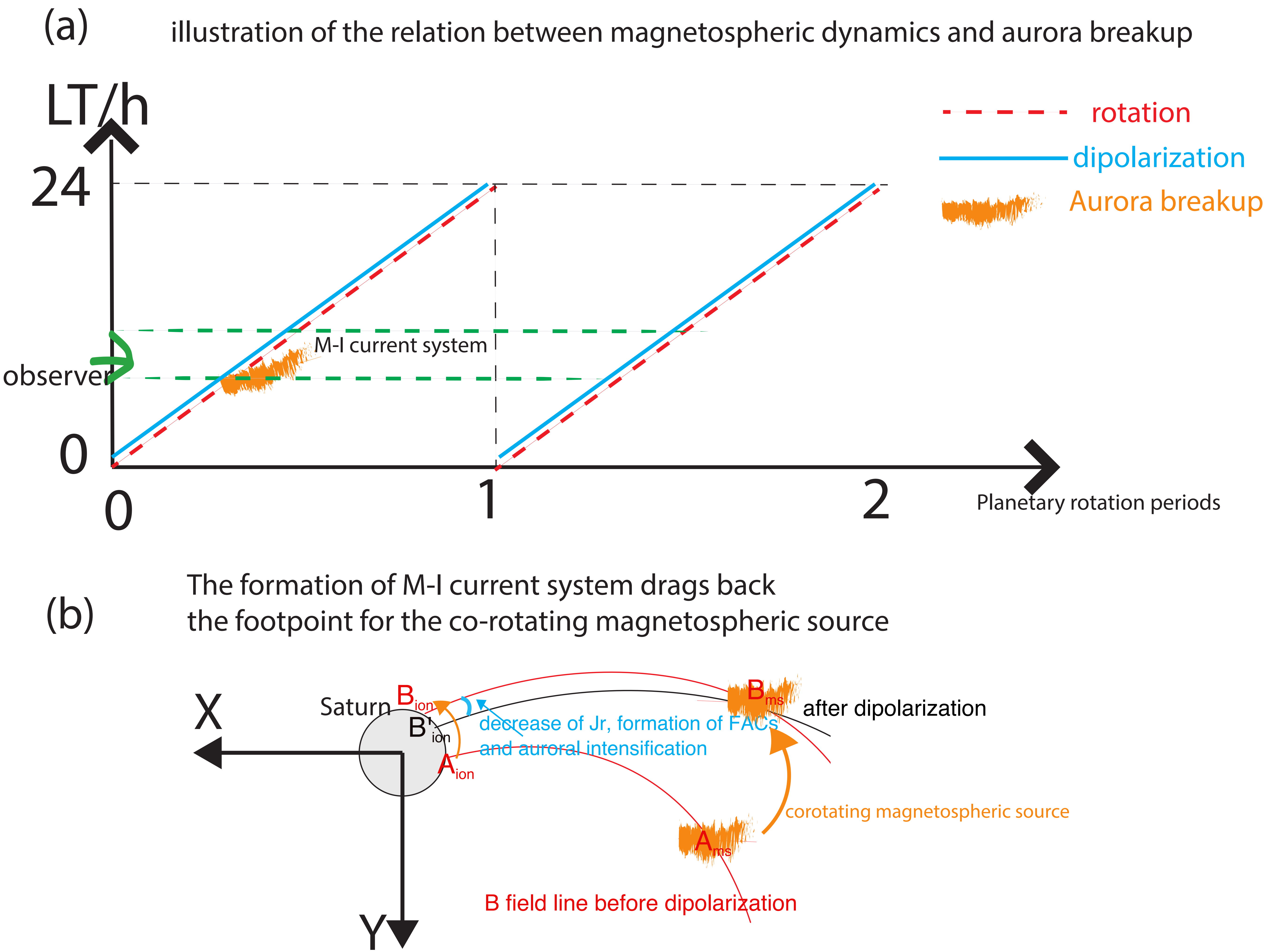
(a)
illustration of the relation between magnetospheric dynamics and aurora breakup
LT/h
24
0
observer
M-I current system
rotation
dipolarization
Aurora breakup
0
1
2
Planetary rotation periods
(b)
The formation of M-I current system drags back
the footpoint for the co-rotating magnetospheric source
X
Y
Saturn
B ion
B' ion
A ion
B ms
A ms
after dipolarization
decrease of Jr, formation of FACs
and auroral intensification
corotating magnetospheric source
B field line before dipolarization